A STUDY IN APPLICATION OF FINITE ELEMENT METHOD TO COMPOSITE PLATES AND SHELLS

by

VENKATESHWAR RAO, A.

DEPARTMENT OF AEROSPACE ENGINEERING

INDIAN INSTITUTE OF TECHNOLOGY KANPUR

APRIL 1990

A STUDY IN APPLICATION OF FINITE ELEMENT METHOD TO COMPOSITE PLATES AND SHELLS

A Thesis submitted

in Partial fulfilment of the Requirements

for the Degree of

MASTER OF TECHNOLOGY

by

VENKATESHWAR RAO, A.

to the

DEPARTMENT OF AEROSPACE ENGINEERING

INDIAN INSTITUTE OF TECHNOLOGY, KANPUR

APRIL, 1990

CERTIFICATE

This is to certify that the work " A STUDY IN APPLICATION OF FINITE ELEMENT METHOD TO COMPOSITE PLATES AND SHELLS " submitted by Venkateshwar Rao. A. in the partial fulfilment of requirements for the degree of Master of Technology has been carried out under my supervision. The work done in this thesis has not been submitted elsewhere for a degree.

April , 1990

V.K. Gupta
Assistant Professor
Department of Aeronautical Engineering
Indian Institute of Technology
Kanpur – 208 016
India

ACKNOWLEDGEMENTS

I express my deep sense of gratitude to Dr.V.K.Gupta for his invaluable guidance, critical supervision and constant encouragement throughout the course of this work. I also wish to express my indebtedness to Dr.P.M.Dixit, who taught me Finite Element Method during the course work.

I sincerely thank my friend C.A.Shankara for his useful suggestions and discussions.

I wish to thank my friends D.S.R.Sharma, Niranjan and A.T.Rao in putting the thesis in to present form.

Thanks are also due to Murthy, Niranjan, Prabhakar, A.T.Rao and Kasi who made my stay here a pleasant one.

Venkateshwar Rao. A

CONTENTS

LIST OF FIGURES

LIST OF TABLES

NOMENCLATURE

a	Dimension of the plate in the x_1 direction
b	Dimension of the plate in the x_2 direction
E_1	Longitudinal elastic modulus for a composite lamina
E_2	Transverse elastic modulus for a composite lamina
G_{12}, G_{13}, G_{23}	Transverse shear modulus for a composite lamina
h	Thickness of the plate
K_1, K_2	Shear correction factors
K_L	Linear stiffness matrix
K_{NL}	Initial displacement matrix
K_σ	Initial stress matrix
K_T	Tangent stiffness matrix
K_G	Geometric stiffness matrix
M_1, M_2, M_6	Moment resultants
N_1, N_2, N_6	Stress resultants
NL	Number of layers in a composite laminate
Q_1, Q_2	Shear resultants
QA, QB, QD, QS	Extensional, Bending-Extensional coupling, Bending Shear stiffness matrix
$\{R_o\}$	Elemental load vector
$\bar{u}_1$, $\bar{u}_2$, $\bar{u}_3$	Displacements in ξ_1, ξ_2, ζ directions
u_1, u_2, u_3	Displacements at the mid plane of the laminate
v	Volume of the laminate
X_1, X_2, X_3	Directions of the cartesian coordinate system
α	Fibre orientation

$\{\delta_i\}$	Displacement vector at the i^{th} node
$\{\epsilon\}^0$	Mid plane strain vector
$\{\epsilon\}^b$	Mid plane curvature vector
$\{\epsilon\}^s$	Mid plane shear strain vector
$\{\epsilon\}^0_L$	Linear mid plane strain vector
$\{\epsilon\}^0_{NL}$	Nonlinear mid plane strain vector
ϕ_1, ϕ_2	Mid plane rotations about ξ_2 and ξ_1 axes respectively
ξ_1, ξ_2, ζ	Curvilinear coordinate system
ν_{12}, ν_{21}	Longitudinal and transverse poisson ratios
$\{\sigma\}$	Stress vector
λ	Buckling load

ABSTRACT

The present work is an attempt to carry out the nonlinear analysis of plates and linear analysis of shells. In both the cases, transverse shear deformation have been included. The nonlinearity is introduced by von-Korman strains. The response is obtained using first order shear deformation theory. Solutions have been obtained using finite element technique. A nine noded doubly curved isoparametric lagrangian finite element is used to d scretize the structure. The results are presented for linear bending, nonlinear bending, linear buckling and postbuckling of plates. However for shells only linear bending and buckling analysis have been conducted.

It is found that the first order theory (FSDT) may involve about 2.5% difference with the higher order theory (HSDT) for a/h = 2 . After a/h = 10 there is hardly any significant difference between FSDT and HSDT which requires lot more computational effort. It is also found out that in case of buckling,FSDT theory gives results which are close to Reddy 's HSDT results for all thickness ratios. This suggests that one need not go for the higher order theory in case of the buckling.

To solve the nonlinear equations in the nonlinear analysi an incremental Newton-Raphson method has been developed which i more efficient than Picard type of iteration. The theoretica results are compared with the experimental results and are foun to be in close agreement. The effect of different simply support

boundary conditions has also been investigated.

Separate programs written in FORTRAN are developed for symmetric and unsymmetric laminates to reduce the computational effort.

CHAPTER 1

INTRODUCTION AND LITERATURE REVIEW

1.1 Introductory Remarks :

In recent years fibre reinforced composites, have found increasing use in many engineering structures and consumer applications, ranging from fuselage of an airplane to the frame of a tennis raquet. This is mainly due to two desirable features of reinforced composites ie., a high strength to weight ratio and flexibility in tailoring the anisotropic material properties by changing the fibre orientation, stacking sequence and thickness of laminae. The increasing use of composites as a structural element has generated considerable interest in the analysis of composite plates and shells.

Composites can be considered as a material consisting of two or more chemically distinct constituents with a distinct interface between them. The properties of composites are noticeably different from constituent materials. Fibrous composites consist of essentially high strength fibres embedded in a matrix. A lamina is a thin sheet with fibers, oriented in certain directions, forming the main load bearing members. The matrix keeps fibres in position and transfers the stress to fibres through bonding. The lamina can be considered to behave as a two dimensional orthotropic material.

The main advantage of composites lies in tailoring the

material properties to suit the applied loads. The disadvantage, from analytical point of view is the existence of coupling between bending and stretching. Due to this the governing partial differential equations for laminae become coupled in displacements and rotations. This boundary value problem is difficult to solve. Very few exact solutions can be obtained for limited boundary conditions. This is a marked departure from conventional isotropic materials.

Due to the high ratio of elastic modulus to shear modulus (of the order of 25 to 40, instead of 2.6 for a typical isotropic material), shear deformation can be significant in composite materials as compared to isotropic materials. The classical plate theory which does not take into account the transverse shear deformation, under predicts the deflections and over predicts the buckling loads and the natural frequencies, when the ratio of lateral dimension to the thickness is less than 50.

For small deflections ie., the deflections which are small compared to thickness, the linear theory gives sufficiently accurate results. Plates, subjected to lateral loads and/or in plane loads, fail at large deflections. For large deflections the lateral deflection is accompanied with mid plane stretching. This increases the load carrying capacity of the plate. Associated increase in load depends on the in plane boundary conditions imposed on the edges. This behavior is extremely important in structural weight minimization in aerospace structures. A plate starts to buckle when the critical load is reached. The maximum stress at the instant of buckling is much lesser than the yield

stress of the material. Hence the plate can take more load. As the in plane load is increased, the deflections increase at a faster rate. Now the deflections are no more comparable with the thickness, violating small deflection theory. Therefore large deflection theory should be considered to determine accurate load carrying capacity of laminated plates.

The rapid development of computing technology has completely changed the out look of structural analyst. Of all approximate methods to analyze the structures, involving complex geometries and variety of boundary conditions, finite element method (FEM) is found to be most powerful. FEM, in structural analysis, is a technique that discretizes a structure in to a set of simple sub domains called finite elements. Over each element the solution of the governing differential equation is approximated by a linear combination of undetermined parameters and pre selected algebraic polynomials. The undetermined parameters are determined such that the variational statement obtained from the governing differential equations is satisfied in each element. The satisfaction of the variational statement results in a set of algebraic relations among the undetermined parameters of an element. Since the domain is divided into a set of elements, they are put together into their original position, called assembly of elements, using continuity at element interface. The finite element method typically entails the solution of a very large number of equations for the nodal values of the function being sought. Thus the method requires so much computation that it is practical only if calculations are carried

on a computer.

In the present work FEM is used to carry out the linear and non linear analysis of composite laminates including transverse shear deformation.

1.2 Literature Review :

The pertinent literature survey is presented here under the following three headings.

(i) Studies using small deflection theory of plates.

(ii) Studies using large deflection theory of plates.

(iii) Studies devoted to small deflection theory of shells.

1.2 (i) Studies Using Small Deflection Theory of Plates :

A number of theories have been proposed for shear deformable laminated plates. Stavsky [1] extended the classical plate theory for isotropic materials to laminated plates. This theory has been generalized to laminated anisotropic plates by Yang, Norris and Stavsky [2] and is called as YNS - theory. This is generalization of the Mindlin plate theory which includes transverse shear deformation and rotary inertia effects. In this theory the normal to the mid plane before deformation remains straight after deformation but not necessarily normal to the mid plane. To make shear strains zero on top and bottom faces of the plate, a shear correction factor is used which depends upon the ply lay-up and fibre orientation, etc. It has been shown that

[3-5] YNS theory predicts the transverse deflections and natural frequencies for laminated composite plates with reasonable accuracy. Whitney and Pagano [6] presented some close form solutions for cross ply and angle ply rectangular plates under sinusoidal loading. Sinha and Rath [7] considered both vibration and buckling for the same type of plates. They investigated the influence of shear deformation, panel curvature and aspect ratio on bending stretching coupling. They used Navier type solution to reduce the governing partial differential equations to algebraic equations.

The finite element analysis of laminated composite plates began with Pryor and Barker [8] who employed twenty eight degree of freedom (dof) shear deformable rectangular element.Pica [9] has compared the results of linear, serendipity, lagrangian and heterosis elements with analytical thin plate solutions for square, circular and elliptical isotropic plates based on YNS theory. He suggested the use of heterosis elements for rectangular and curved element meshes. Reddy [10] developed C^0 penalty plate bending element based on YNS theory. The element consists of five dof at each node- three displacements and two rotations at the mid plane of the plate. Reddy [11] presented comparison of the finite element solutions using penalty method and exact solutions for anisotropic plates. He used reduced integration to correct the shear stiffness. He concluded that higher order elements are not affected by locking. He showed that nine noded lagrangian element is not much affected by the integration scheme but eight noded element is profoundly affected. The consideration of symmetries in

unsymmetrical laminated composite plates was investigated by Reddy [12]. He presented the boundary conditions to be used in full and quarter plate models of cross ply and angle ply laminated plates. Hass and Lee [13] used a nine noded degenerate shell element based on modified Hellinger Reissiner principle. Functions were assumed independently for in plane and transverse shear strains.

The finite element formulation for the isotropic plate buckling, using classical theory, is available in standard texts [14,15]. Gajbir Singh and Sadasiva Rao [22] used an eight noded Mindlin element for the stability analysis of thick angle ply laminates. The effect of fibre orientation, material properties, layering and boundary conditions on buckling loads were studied.

Further development in laminate analysis have been higher order theories. Phan and Reddy [16] presented a higher order theory where in plane displacements are expanded as cubic function of the thickness coordinate while the transverse deflection is kept constant over the thickness of the plate. They presented closed form solutions for the bending of symmetric cross-ply laminates. Recently Phan and Reddy [17] using the higher order theory presented closed form solutions for the stability of isotropic, orthotropic and laminated plates.

1.2 (ii) Studies Using Large Deformation Theory of Plates :

Much of research in the laminated composite plates is limited to linear problems. This is due to the complexity of non linear partial differential equations associated with large

deflection theory of composite plates. Approximate solutions for composite plates using large deflection theory based on Von Korman theory of isotropic plates have been attempted by [23-24]. Chandra and Raju [23] and Chia and Prabhakara [24] employed the gelerkian method to reduce the governing differential equations to an ordinary differential equation, in time for the mode shape. The perturbation technique was used to solve the resulting equations. They analyzed bending and free vibration of composite laminates.

Using FEM the total stiffness matrix can be written as the sum of linear stiffness matrix and non linear stiffness matrix. The non linear stiffness matrix is called as incremental stiffness matrix. Two notations have emerged for the incremental matrices formulated in total lagrangian system. In total lagrangian system all the quantities of interest are expressed as functions of rectangular co-ordinates of the body in its initial or undeformed state. The first notation is due to Mallet and Marcal [25] and will be referred to as [N] notation. In this type of formulation, the expressions for total energy, and equilibrium are expressed as

$$\Pi = \{q\}^T \left(\frac{1}{2} [K]_L + \frac{1}{6} [N1] + \frac{1}{12} [N2] \right) \{q\} - \{q\}^T \{R\}$$

$$\left([K]_L + \frac{1}{2} [N1] + \frac{1}{3} [N2] \right) \{q\} = \{R\} \qquad (1.1)$$

Where K_L is the linear stiffness matrix and elements of N1 and N2 depend linearly and quadratically on the transverse

deflection u_3.

The incremental equilibrium equations can be written as

$$\left([K]_L + [N1] + [N2] \right) \{\delta q\} = \{\Delta R\} \qquad (1.2)$$

The second notation is due to Zienkiwicz and Nayak [26] referred to as [B] notation In this type of formulation the equilibrium equation written as

$$\left([K]_L + [K]_{NL} + [K]_\sigma \right) \{q\} = \{R\} \qquad (1.3)$$

where K_L is the linear stiffness K_{NL} is unsymmetric stiffness matrix and K_σ is the initial stress matrix, due to large deformation theory.

The incremental equilibrium equations can be written as

$$[K]_T \{q\} = \{\Delta R\} \qquad (1.4)$$

where K_T is the tangent stiffness matrix. The various matrices K_L, K_{NL}, K_σ and K_T are derived for first order shear deformation theory in chapter 3.

The correlation between the two notations was presented by Wood [27].

Reddy and Chao [28] used mixed finite element for non

linear bending of composite plates in total Lagrangian system. Putcha and Reddy [29] used mixed finite element for the non linear analysis of laminated plates based on higher order deformation theory. They used Picard type of iteration to solve the non linear algebraic equations with small load increments.

1.2 (iii) Studies Devoted to Small Deflection Theory of Shells :

The analysis of laminated composite shells began with Ambartsumyan [30] . He assumed that individual layers are oriented so that principal axes of material symmetry are coincident with the principal coordinates of shell reference. Dong, Pister and Taylor [31] formulated a theory for laminated shells which is an extension of the developed by Stavsky [1]. His work can be called as Donnel's shallow shell theory. Cheng and Ho [32] analyzed laminated anisotropic shells using Flugge's shell theory [33]. The theory which considers shear deformation and thermal expansion through the thickness was considered by Zukas and Vinson [34].

The finite element analysis of composite shells was attempted by Pandya and Natarajan [35] and Shivakumar and Krishnamurthy [36] and Rao K.P. [37] based on Kirchoff's theory. Pandya and Natarajan [35] used a three noded one dimensional curved finite element having four degrees freedom at each node for the analysis of axisymmetric fibre reinforced laminated shells, subjected to axisymmetric loading. The results for a cylindrical tube subjected to internal pressure and axial tension, are compared with the analytical solution. Shivakumar and

Krishnamurthy [36] used eight dof and sixteen dof ring element for free vibration analysis of laminated cylindrical and conical shells. They showed that for the same number of unknowns results with sixteen dof ring element are in good agreement with the experimental results than eight dof element.

Reddy [38] developed shear deformable finite element for composite shells based on Sander's theory [19]. He compared the approximate shell theories of Love , Sander, Donnel, Morely and Loo. He concluded that the effect of shear deformation on the non dimensional deflections is more pronounced with the decrease in layers. He showed that there is a small difference in results obtained with different shell theories for shallow shells (R/h > 100). But for R/h = 10,the difference in the results obtained with different shell theories is noticeable. Using Von Korman strains and Sander's theory, and incorporating transverse shear deformation, Reddy et.al.[40] presented geometric non-linear analysis of doubly curved shells.

1.3 Aim and Scope of Present Work :

The literature survey presented reveals the necessity of nonlinearity and shear deformation in the composite plates. There are some higher order theories proposed till now to improve the solution accuracy for the linear problems. These are computationally expensive and involve large number of nodal degree of freedom. The analytical methods can be applied to linear problems with limited boundary conditions. But they are not

tractable for nonlinear problems.

The scope of the present study can be summarised below

In Ref. [11] it is stated that higher order elements are not much effected by locking and nine noded lagrangian element is superior than eight noded element. Therefore the present study is an attempt to study the analysis of plates and shells using nine noded shear deformable element. The displacement functions require C^0 continuity which leads to easy formulation for thick and thin plates.

To compare the numerical reliability and numerical accuracy of the first order shear deformation theory [FSDT] compared to higher order theory [HSDT] for linear bending and buckling problems. The FSDT is computationally inexpensive and easy to implement compared to HSDT.

To check the validity of the Von-Korman nonlinear theory, the theoretical results are compared with the experimental results.

A picard type of iteration is used in most of the works in solving the nonlinear equations [28,29]. This type of iteration is computationally expensive. Therefore incremental Newton-Raphson method has been developed.

In the nonlinear analysis the effect of different in plane boundary conditions is significant. The effect is more pronounced with bending-stretching coupling. Hence the nonlinear analysis of two layer cross-ply and two layer angle-ply with S1,S2 and S3 boundary conditions given in chapter 2 is studied.

1.4 Layout of the Thesis :

The thesis has been divided in to five chapters. The first chapter is an introduction to the problem with the pertinent literature.

The second chapter deals with the theoretical formulation and derivation of the expressions which can be readily used in the finite element formulation. THe finite element formulation and the solution procedure is presented in chapter 3. Chapter 4 deals with the interpretation of the results obtained and is followed by conclusions and scope of further work in chapter 5.

The thesis has Appendix-I and Appendix-II. The figures and tables are given in the chapters that follow as and when the need arises.

CHAPTER 2

THEORETICAL FORMULATION

2.1 Introduction :

This chapter presents a detailed formulation of shear deformation theory of shells based on Sanders theory, including geometric nonlinearity. The geometric nonlinearity is introduced by von-Korman strains. The nonlinear partial differential equations for plates and shells cannot be solved analytically for complex geometries and various boundary conditions. FEM is the most effective numerical method to solve such problems.

FEM is a piece wise application of variational method. In variational method the governing differential is recast in an equivalent integral form and a variational formulation is derived. This results weaker continuity requirements on the solution in the variational problem than in the original equation.

In solid mechanics problems the variational form of the governing equations represents the total potential energy of the system. The solution of the differential equation is found by minimizing the variational form with respect to unknown variables. For monotonic convergence the primary variable should be continuous up to one order less than highest order, occurring in the variational functional.

The classical plate requires cubic or higher order interpolation functions for approximating transverse deflection. But this first order shear deformation theory allows us to use linear or higher order interpolation functions for all

displacements. This type of formulation is easy to implement and applicable for both thin and thick laminates. However, shear deformable elements suffer from locking phenomenon. It is necessary that the shear strain fields, as the plate thickness reduces, should satisfy the Kirchoff's condition ie.,

$$\gamma_{xz} = \phi_x + w_{,x} \longrightarrow 0$$

and $$\gamma_{yz} = \phi_y + w_{,y} \longrightarrow 0$$

Conventional methods using exact integration fails to do this consistently, introducing spurious constraints that lead to locking and severe stress oscillations. Therefore reduced integration technique is used to circumvent the locking.

2.2 Assumptions made in the Theory :

Theoretical development in the present work is based upon the following assumptions.

(i) The laminate is constructed of an arbitrary number of layers of orthotropic sheets bonded together. However the orthotropic axis of material symmetry of an individual layer need not coincide with the laminated coordinate system.

(ii) The strains are small.

(iii) The transverse normal stress and strain are negligible.

(iv) The line normal to the mid plane after deformation remains straight but not necessarily normal to the mid plane.

(v) There are no body forces.

(vi) Stress-strain relations are linear.

2.3 Shell Geometry :

Fig.2.1 shows a differential element of a shell. Here (ξ_1, ξ_2, ζ) denote curvilinear coordinates such that ξ_1 and ξ_2 curves are lines of curvature on the mid surface $\zeta = 0$. The ζ curves are straight lines perpendicular to surface $\zeta = 0$. The lines of principal radii of curvature coincide with the coordinate lines and the values are denoted by R_1 and R_2. X_1 and X_2 denote cartesian reference frame.

The linear displacement field is given by,

$$\begin{aligned} \bar{u}(\xi_1, \xi_2, \zeta) &= u_1(\xi_1, \xi_2, 0) + \zeta \phi_1 \\ \bar{v}(\xi_1, \xi_2, \zeta) &= u_2(\xi_1, \xi_2, 0) + \zeta \phi_2 \\ \bar{w}(\xi_1, \xi_2, \zeta) &= u_3(\xi_1, \xi_2, 0) \end{aligned} \qquad (2.1)$$

Where $\bar{u}$, $\bar{v}$, $\bar{w}$ are the displacements along (ξ_1, ξ_2, ζ) coordinates, u_1, u_2, u_3 are the displacements of the corresponding point on the middle surface and ϕ_1 and ϕ_2 are the rotations at $\zeta = 0$ about ζ_2 and ζ_1 axis respectively.

The strain displacement relations including geometric nonlinearity can be written as

$$\begin{aligned} \epsilon_1 &= \epsilon_1^o + \zeta\ k_1^o \\ \epsilon_2 &= \epsilon_2^o + \zeta\ k_2^o \\ \epsilon_4 &= \epsilon_4^o \\ \epsilon_5 &= \epsilon_5^o \\ \epsilon_6 &= \epsilon_6^o + \zeta\ k_6^o \end{aligned} \qquad (2.2)$$

Where ϵ_i^o and k_i^o are the mid plane strains and curvatures respectively. They can be written as [40]

$$\epsilon_1^o = \frac{\partial u_1}{\partial x_1} + \frac{u_3}{R_1} + \frac{1}{2}\left(\frac{\partial u_3}{\partial x_1}\right)^2 \quad ; \quad k_1^o = \frac{\partial \phi_1}{\partial x_1}$$

$$\epsilon_2^o = \frac{\partial u_2}{\partial x_2} + \frac{u_3}{R_2} + \frac{1}{2}\left(\frac{\partial u_3}{\partial x_2}\right)^2 \quad ; \quad k_2^o = \frac{\partial \phi_2}{\partial x_2}$$

$$\epsilon_6^o = \frac{\partial u_1}{\partial x_2} + \frac{\partial u_2}{\partial x_1} + \left(\frac{\partial u_3}{\partial x_1}\right)\left(\frac{\partial u_3}{\partial x_2}\right) \quad ; \quad k_6^o = \frac{\partial \phi_1}{\partial x_2} + \frac{\partial \phi_2}{\partial x_1} - C_o\left(\frac{\partial u_2}{\partial x_1} - \frac{\partial u_1}{\partial x_2}\right)$$

$$\epsilon_4^o = \phi_2 + \frac{\partial u_3}{\partial x_2} - \frac{u_2}{R_2}$$

$$\epsilon_5^o = \phi_1 + \frac{\partial u_3}{\partial x_1} - \frac{u_1}{R_1} \qquad \text{.(2.3a)}$$

Where

$$C_o = \frac{1}{2}\left(\frac{1}{R_1} - \frac{1}{R_2}\right) \qquad \text{(2.3b)}$$

The term C_o is due to Sander's theory which accounts for the condition of zero strain for rigid body motion.

2.4 Stress-Strain Relations for a Lamina :

First order shear deformation theory used in the present work is incapable of satisfying the condition of zero transverse strain on top and bottom surfaces. Correction factors K_1 and K_2 have been used to account for this in stress strain relations.

Based on the assumption that the transverse stress σ_3 is negligible, the stress strain relations for an orthotropic lamina k oriented arbitrarily to the laminate axis are given by

$$\begin{Bmatrix} \sigma_1 \\ \sigma_2 \\ \sigma_6 \\ \sigma_4 \\ \sigma_5 \end{Bmatrix}_k = \begin{bmatrix} \bar{Q}_{11} & \bar{Q}_{12} & \bar{Q}_{16} & 0 & 0 \\ & \bar{Q}_{22} & \bar{Q}_{26} & 0 & 0 \\ & & \bar{Q}_{66} & 0 & 0 \\ & & & K_1^2\,\bar{Q}_{44} & K_1K_2\,\bar{Q}_{45} \\ & & & & K_2^2\,\bar{Q}_{44} \end{bmatrix}_k \begin{Bmatrix} \epsilon_1 \\ \epsilon_2 \\ \epsilon_6 \\ \epsilon_4 \\ \epsilon_5 \end{Bmatrix} \quad (2.4)$$

Eqn.(2.4) can be written in more compact notation as

$$\{\sigma\}_k = [\bar{Q}]_k \{\epsilon\}$$

Expressions for the elements of $[\bar{Q}]$ matrix in terms of engineering constants for lamina for a given orientation α are given in Appendix-I.

2.5 Stress-Resultants at the Mid Plane of the Laminate :

The stress resultants N_1, N_2, N_6, M_1, M_2, M_6, Q_1 and Q_2 of the laminate with NL number of layers is given by

$$(N_1, N_2, N_6) = \sum_{L=1}^{NL} \int_{\zeta_K}^{\zeta_{K+1}} (\sigma_1, \sigma_2, \sigma_6)\, d\zeta$$

$$(M_1, M_2, M_6) = \sum_{L=1}^{NL} \int_{\zeta_K}^{\zeta_{K+1}} (\sigma_1, \sigma_2, \sigma_6)\, \zeta \quad d\zeta \qquad (2.5)$$

$$(Q_1, Q_2) = \sum_{L=1}^{NL} \int_{\zeta_K}^{\zeta_{K+1}} (\sigma_4, \sigma_5)\, d\zeta$$

The stress resultants are as shown in Fig.2.2.

Substituting relations (2.2) in Eqn.2.4 the following expressions for stresses are obtained

$$\begin{Bmatrix} \sigma_1 \\ \sigma_2 \\ \sigma_6 \end{Bmatrix} = \begin{bmatrix} \bar{Q}_{11} & \bar{Q}_{12} & \bar{Q}_{16} \\ & \bar{Q}_{22} & \bar{Q}_{26} \\ \text{Sym} & & \bar{Q}_{66} \end{bmatrix} \begin{Bmatrix} \epsilon_1^o \\ \epsilon_2^o \\ \epsilon_6^o \end{Bmatrix} + \begin{bmatrix} \bar{Q}_{11} & \bar{Q}_{12} & \bar{Q}_{16} \\ & \bar{Q}_{22} & \bar{Q}_{26} \\ \text{Sym} & & \bar{Q}_{66} \end{bmatrix} \zeta \begin{Bmatrix} k_1^o \\ k_2^o \\ k_6^o \end{Bmatrix}$$

$$\begin{Bmatrix} \sigma_4 \\ \sigma_5 \end{Bmatrix} = \begin{bmatrix} K_1^2 \bar{Q}_{44} & K_1 K_2 \bar{Q}_{45} \\ & K_2^2 Q_{55} \end{bmatrix} \begin{Bmatrix} \epsilon_4^\circ \\ \epsilon_5^\circ \end{Bmatrix} \qquad (2.6)$$

Rewriting the stress resultants (2.5) in terms of mid plane strains and curvatures after integrating through each layer

$$\begin{Bmatrix} N_1 \\ N_2 \\ N_6 \\ M_1 \\ M_2 \\ M_6 \end{Bmatrix} = \left[\begin{array}{c:c} [QA] & [QB] \\ \hdashline \text{Sym} & [QD] \end{array}\right] \begin{Bmatrix} \epsilon_1^\circ \\ \epsilon_2^\circ \\ \epsilon_6^\circ \\ k_1^\circ \\ k_2^\circ \\ k_6^\circ \end{Bmatrix} \qquad (2.7)$$

$$\begin{Bmatrix} Q_4 \\ Q_5 \end{Bmatrix} = \begin{bmatrix} QS \end{bmatrix} \begin{Bmatrix} \epsilon_4^\circ \\ \epsilon_5^\circ \end{Bmatrix}$$

Where QA, QB, QD and QS are extensional, bending - extensional coupling, bending, and shear stiffness matrices respectively. They are given by,

$$\left([QA], [QB], [QD] \right) = \sum_{L=1}^{NL} \int_{\zeta_K}^{\zeta_{K+1}} [\bar{Q}] \left(1, \zeta, \zeta^2 \right) d\zeta$$

$$i = j = 1,3,6 \qquad (2.8)$$

$$[QS] = \sum_{L=1}^{NL} \int_{\zeta_K}^{\zeta_{K+1}} [\bar{Q}] \, d\zeta$$

$$i = j = 4,5 \qquad (2.9)$$

2.6 Boundary conditions :

Since displacement based formulation is used in the present study only displacement boundary condition has to be specified. One can develop Navier solutions for different types of laminates with three types of simply supported boundary conditions. They are referred in this thesis as S1, S2 and S3 respectively.

The functions which satisfy S1 boundary conditions are

$$
\begin{aligned}
u_1(x_1,x_2) &= \sum_{n=1} \sum_{m=1} U_{mn} \cos \alpha x_1 \sin \beta x_2 \\
u_2(x_1,x_2) &= \sum_{n=1} \sum_{m=1} V_{mn} \sin \alpha x_1 \cos \beta x_2 \\
u_3(x_1,x_2) &= \sum_{n=1} \sum_{m=1} W_{mn} \sin \alpha x_1 \sin \beta x_2 \\
\phi_1(x_1,x_2) &= \sum_{n=1} \sum_{m=1} X_{mn} \cos \alpha x_1 \sin \beta x_2 \\
\phi_2(x_1,x_2) &= \sum_{n=1} \sum_{m=1} Y_{mn} \sin \alpha x_1 \cos \beta x_2
\end{aligned}
\qquad (2.10)
$$

$$
N_1(o,x_2) = N_1(a,x_2) = N_2(x_1,o) = N_2(x_1,b) = 0
$$

$$
M_1(o,x_2) = M_1(a,x_2) = M_2(x_1,o) = M_2(x_1,b) = 0
$$

Where $\alpha = \frac{m\pi}{a}$ and $\beta = \frac{n\pi}{b}$, a and b are plane form dimensions of the shell.

The expressions which satisfy S2 boundary conditions are

$$
\begin{aligned}
u_1(x_1,x_2) &= \sum_{n=1} \sum_{m=1} U_{mn} \sin \alpha x_1 \cos \beta x_2 \\
u_2(x_1,x_2) &= \sum_{n=1} \sum_{m=1} V_{mn} \cos \alpha x_1 \sin \beta x_2
\end{aligned}
$$

$$
N_6(o,x_2) = N_6(a,x_2) = N_6(x_1,o) = N_6(x_1,b) = 0
$$

$$
M_1(o,x_2) = M_1(a,x_2) = M_2(x_1,o) = M_2(x_1,b) = 0
$$

The remaining expressions are same as given in Eqn.2.8

The boundary conditions S1, S2 and S3 for full shell and quarter shell for m = n = 1 are as shown in Fig.2.3

For clamped case all the displacements and rotations are restrained at the edge ie.,

$$u_1 = u_2 = u_3 = \phi_1 = \phi_2 = 0 \qquad (2.11)$$

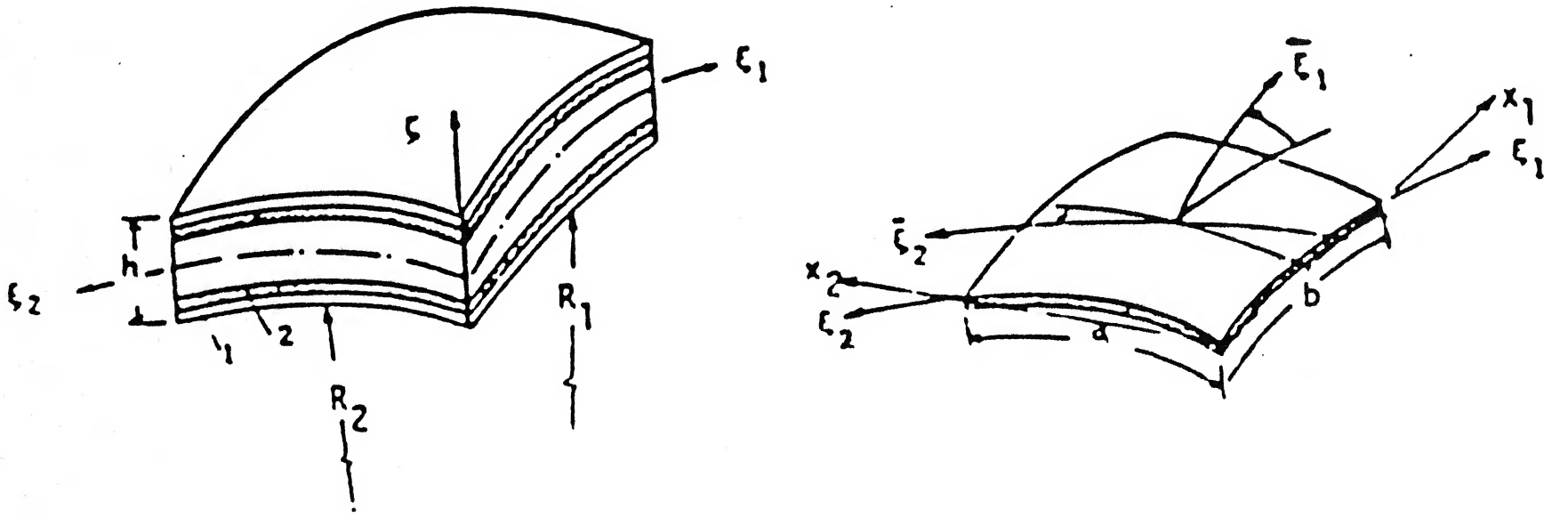

Fig. 2.1 Laminated shell geometry and lamina details

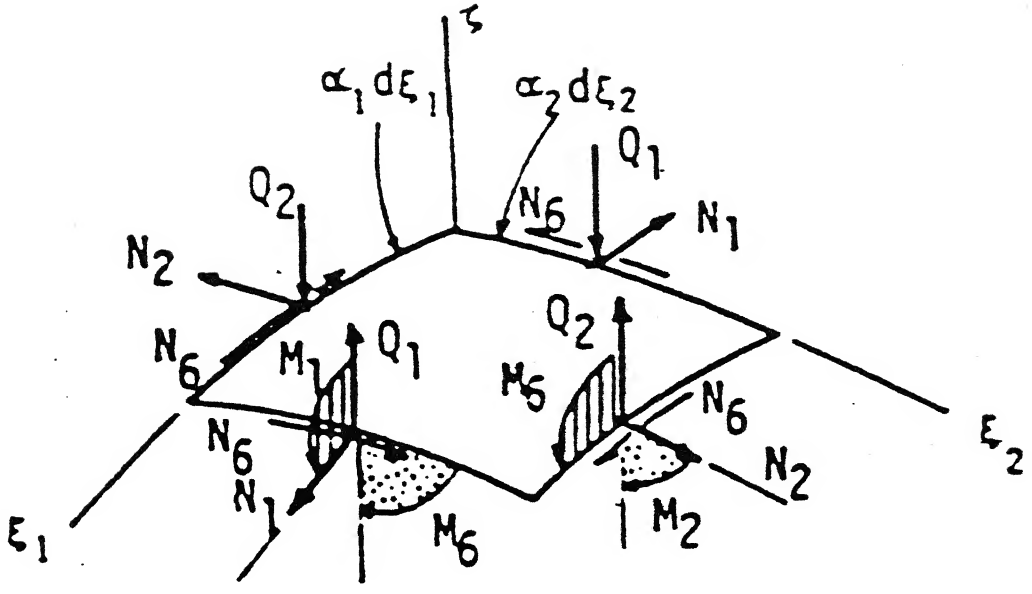

Fig. 2.2 Stress resultants of a shell

S1 :

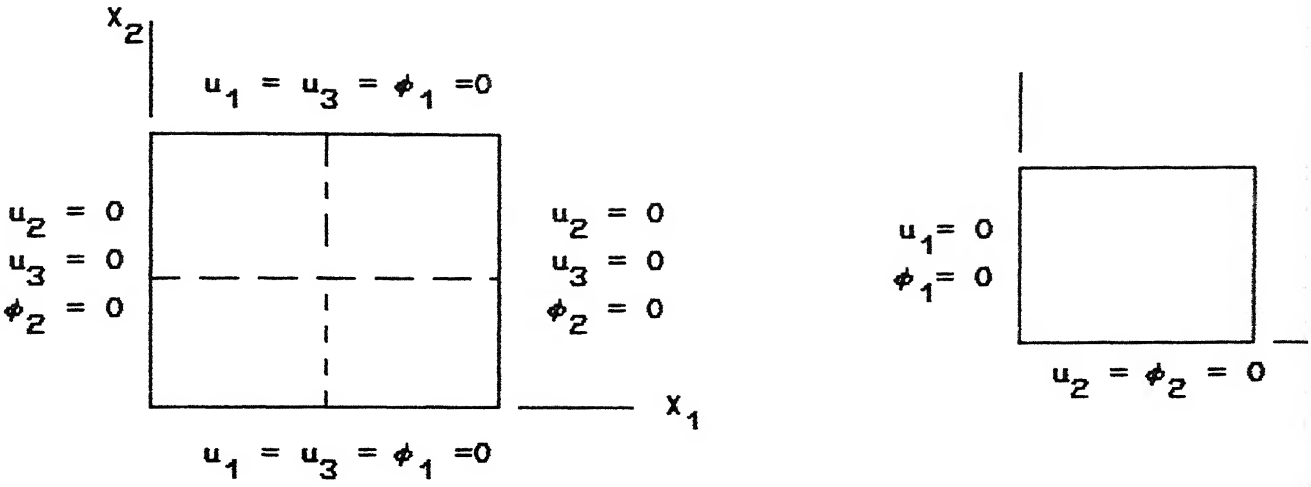

S2 :

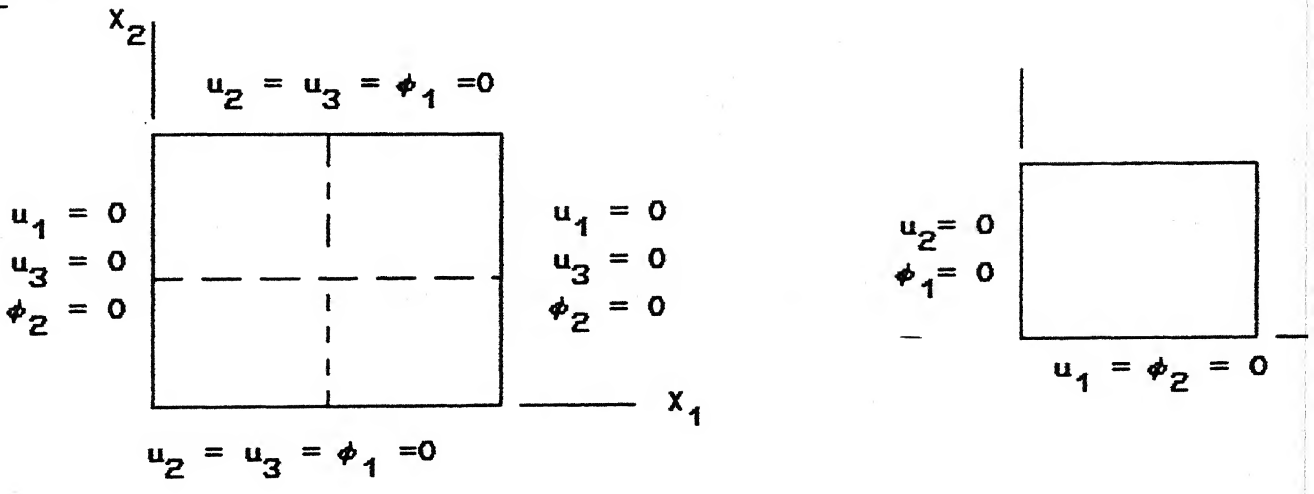

S3 :

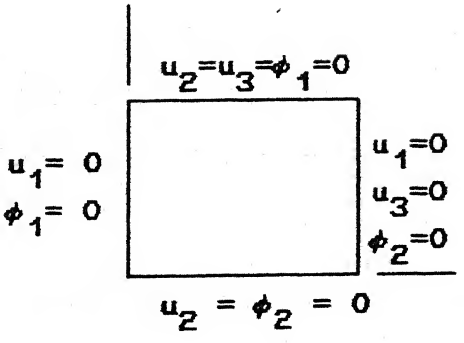

Fig. 2.3 Simply supported boundary conditions used in the present study

CHAPTER 3

FINITE ELEMENT FORMULATION AND SOLUTION PROCEDURE

3.1 Introduction :

In this chapter a displacement finite element formulation, based on total lagrangian for nonlinear analysis is presented. The continuum is divided in to number of elements and over each element a set of functions are chosen to define the state of displacements. The total potential energy is written in terms of displacements and using the principle of stationary of total potential for an element, we obtain equations which are nonlinear. These equations are solved by Newton-Raphson method.

3.2 Element :

The element used in the present work is a shear deformable, doubly curved shell element whose projection is an isoparametric rectangular element on ξ_1, ξ_2 plane. Over the typical shell element A , the displacements u_1, u_2, u_3, ϕ_1 and ϕ_2 are interpolated by the expressions of the form

$$u_i = \sum_{J=1}^{NN} N_J (\xi_1, \xi_2) \; u_i^J \qquad i = 1,3 \qquad (3.1a)$$

$$\phi_i = \sum_{J=1}^{NN} N_J \ (\xi_1, \xi_2) \ \phi_i^{J\,e} \qquad i = 1,2 \qquad (3.1b)$$

Where NN is the number of nodes (9), N_J is the shape functions associated with node J and $u_i^{J\,e}$, $\phi_i^{J\,e}$ are the unknown nodal variables. The shape functions are given in [14]

3.3 Total Lagrangian Virtual Work Equation :

The basis of the present formulation is the virtual work equation for a continuum written in total lagrangian coordinate system under the assumption of small strains.

$$\int_V d\epsilon_i^T \sigma_i \, dv = \int_V \rho \, du_j^T q_j \, dv + \int_A du_j^T R_j \, dA \qquad \begin{matrix} i=1,5 \\ j=1,3 \end{matrix} \qquad (3.2)$$

Where v is the undeformed volume, ρ is the mass density, q_j is the body force per unit mass and R_j is the surface tractions per unit area, acting over the undeformed area. Here symbol d is used to denote first variation.

The internal virtual work $d W_i^e$ over a element is given by,

$$d W_I^e = \int_{V^e} d\epsilon_i^T \sigma_i \, dv \qquad (3.3a)$$

$$d W_I^e = \int_A \int_{-h/2}^{h/2} d \epsilon_i^T \sigma_i \, d\zeta \, dA \qquad (3.3b)$$

Substituting the strain relations Eqn.(2.2) in to Eqn.(3.3b), we obtain,

$$dW_I^e = \int_A \int_{-h/2}^{h/2} \Big[d(\epsilon_1^o + \zeta k_1^o) \sigma_1 + d(\epsilon_2^o + \zeta k_2^o) \sigma_2 + d(\epsilon_6^o + \zeta k_6^o) \sigma_6 + d \epsilon_4^o \sigma_4 + d \epsilon_5^o \sigma_5 \Big] d\zeta \, dx_1 \, dx_2 \qquad (3.4)$$

Where h is the thickness of the laminate. After integrating through the thickness of the laminate, Eqn.3.4 can be written as

$$dW_i^e = \int_A \Big[N_1 \, d \epsilon_1^o + M_1 \, dk_1^o + N_2 \, d \epsilon_2^o + M_2 \, dk_2^o + N_6 \, d \epsilon_6^o + M_6 \, dk_6^o + Q_1 \, d \epsilon_4^o + Q_2 \, d \epsilon_5^o \Big] dx_1 \, dx_2 \qquad (3.5)$$

Defining the mid plane strains, bending strains and shear strains in a matrix form as,

$$\left\{ \epsilon \right\}^{o^T} = \left\{ \epsilon_1^o, \ \epsilon_2^o, \ \epsilon_6^o \right\}$$

$$\left\{ \epsilon \right\}^{b^T} = \left\{ k_1^o, \ k_2^o, \ k_6^o \right\} \qquad (3.6)$$

$$\left\{ \epsilon \right\}^{s^T} = \left\{ \epsilon_4^o, \ \epsilon_5^o \right\}$$

The mid plane strain ϵ_i^o can be written as sum of linear strain and nonlinear strain. The linear strain is due to membrane strain and the nonlinear strain is due to bending deformation u_3 only.

$$\left\{ \epsilon \right\}^o = \left\{ \epsilon \right\}_L^o + \left\{ \epsilon \right\}_{NL}^o \qquad (3.7a)$$

Where

$$\left\{ \epsilon \right\}_L^o = \begin{Bmatrix} \dfrac{\partial u_1}{\partial x_1} + \dfrac{u_3}{R_1} \\ \dfrac{\partial u_2}{\partial x_2} + \dfrac{u_3}{R_2} \\ \dfrac{\partial u_1}{\partial x_2} + \dfrac{\partial u_2}{\partial x_1} \end{Bmatrix} \ ; \ \left\{ \epsilon \right\}_{NL}^o = \begin{Bmatrix} \frac{1}{2} \left(\dfrac{\partial u_3}{\partial x_1} \right)^2 \\ \frac{1}{2} \left(\dfrac{\partial u_3}{\partial x_2} \right)^2 \\ \left(\dfrac{\partial u_3}{\partial x_1} \right) \left(\dfrac{\partial u_3}{\partial x_2} \right) \end{Bmatrix} \qquad (3.7b)$$

3.3.1 Expression For $d\left\{\epsilon\right\}_L^o$:

The membrane strain $\left\{\epsilon\right\}_L^o$ can be written in a matrix form in

terms of unknown nodal displacements. Using the Eqn.(3.1) in Eqn.(3.7b) one gets

$$\left\{\epsilon\right\}_L^0 = \left[\ B\ \right]_L^{0\,e} \left[\ \delta\ \right]^e \qquad (3.8a)$$

Here $\left[\ B\ \right]_L^{0\,e}$ is a matrix of size 3x45 and is given below

$$\left[\ B\ \right]_L^{0\,e} = \left[\ B_{01},\ B_{02},\ - - - - - - - - - B_{09}\ \right]_L^e \qquad (3.8b)$$

B_{0j} are the sub matrices and is given by,

$$\left[\ B\ \right]_{0jL}^e = \begin{bmatrix} \frac{\partial N_j^e}{\partial x_1} & 0 & \frac{N_j^e}{R_1} & 0 & 0 \\ 0 & \frac{\partial N_j^e}{\partial x_2} & \frac{N_j}{R_2} & 0 & 0 \\ \frac{\partial N_j^e}{\partial x_2} & \frac{\partial N_j^e}{\partial x_1} & 0 & 0 & 0 \end{bmatrix} \qquad (3.8c)$$

$\left\{\delta^e\right\}$ represents column vector containing unknown nodal displacements and is given below

$$\left\{\ \delta^e\right\}^T = \left\{\ \delta_1,\ \delta_2,- - - - - - - - - - - - \delta_9\ \right\}^{e^T}$$

and

$$\left\{\ \delta_J\right\}^T = \left(\ u_1,\ u_2,\ u_3,\ \phi_1,\ \phi_2\ \right)^J \qquad (3.8d)$$

The matrix $\left[\ B\ \right]_L^{0\,e}$ does not involve the nodal degree of freedom. Therefore the first variation of the linear membrane strain can be written as

$$d\left\{ \epsilon \right\}_L^o = \left[B \right]_L^{oe} \left[d\,\delta \right]^e \qquad (3.9)$$

3.3.2. Expression for $d\left\{ \epsilon \right\}_{NL}^o$

Rewriting the Eqn. (3.7b)

$$\left\{ \epsilon \right\}_{NL}^o = \frac{1}{2} \begin{bmatrix} \frac{\partial u_3}{\partial x_1} & 0 \\ 0 & \frac{\partial u_3}{\partial x_2} \\ \frac{\partial u_3}{\partial x_2} & \frac{\partial u_3}{\partial x_1} \end{bmatrix} \begin{Bmatrix} \frac{\partial u_3}{\partial x_1} \\ \frac{\partial u_3}{\partial x_2} \end{Bmatrix} \qquad (3.10a)$$

This nonlinear mid plane strain can be written in terms of nodal dof as,

$$\left\{ \epsilon \right\}_{NL}^o = \frac{1}{2} \left[E \right]^e \left[G \right]^e \left\{ \delta \right\}^e \qquad (3.10b)$$

Where

$$\left[G \right]^e = \left[G_1, G_2 - - - - - - - G_9 \right] \qquad (3.10c)$$

and

$$\left[G_J \right]^e = \begin{bmatrix} 0 & 0 & \frac{\partial N_J^e}{\partial x_1} & 0 & 0 \\ 0 & 0 & \frac{\partial N_J^e}{\partial x_2} & 0 & 0 \end{bmatrix} \qquad (3.10d)$$

The equation (3.10b) can be rewritten as

$$\left\{\epsilon\right\}_{NL}^{o} = \frac{1}{2}\left[\,B\,\right]_{NL}^{o^{e}}\left[\,\delta\,\right]^{e} \qquad (3.11a)$$

where $\left[\,B\,\right]_{NL}^{o^{e}} = \left[\,B_{01}, B_{02} - - - - - - - - B_{09}\,\right]_{NL}^{e}$ (3.11b)

and

$$\left[\,B_{0J}\right]_{NL}^{e} = \begin{bmatrix} 0 & 0 & \left(\frac{\partial u_3}{\partial x_1}\right)\left(\frac{\partial N_J^e}{\partial x_1}\right) & 0 & 0 \\ 0 & 0 & \left(\frac{\partial u_3}{\partial x_2}\right)\left(\frac{\partial N_J^e}{\partial x_2}\right) & 0 & 0 \\ 0 & 0 & \left(\frac{\partial u_3}{\partial x_1}\right)\left(\frac{\partial N_J^e}{\partial x_2}\right) + \left(\frac{\partial u_3}{\partial x_2}\right)\left(\frac{\partial N_J^e}{\partial x_1}\right) & 0 & 0 \end{bmatrix} \qquad (3.11c)$$

The first variation of nonlinear mid plane strain can be written as

$$d\left\{\epsilon\right\}_{NL}^{o} = \frac{1}{2}\left[\left[\,B\,\right]_{NL}^{o^{e}}\left\{d\,\delta\right\}^{e} + d\left[\,B\,\right]_{NL}^{o^{e}}\left\{\delta\right\}^{e}\right] \qquad (3.12)$$

In $\left[\,B\,\right]_{NL}^{o^{e}}$ matrix, the term u_3 is expressed in terms of shape functions. After applying variation and rearranging the terms we obtain as,

$$\left[\;d\left[\,B\,\right]_{NL}^{o^{e}}\left\{\delta\right\}^{e}\;\right] = \left[\;\left[\,B\,\right]_{NL}^{o^{e}}\left\{d\,\delta\right\}^{e}\;\right] \qquad (3.13)$$

Substituting the relation (3.13) in to (3.12) gives,

$$d\left\{ \epsilon \right\}^{o}_{NL} = \left[B \right]^{o^{e}}_{NL} \left\{ d\delta \right\}^{e} \qquad (3.14)$$

3.3.3 Expression for First Variation of Total Mid Plane Strain :

The first variation of total mid plane strain can be written using relations (3.9) and (3.14) as,

$$d\left\{ \epsilon \right\}^{o} = \left[B \right]^{o^{e}} \left\{ d\delta \right\}^{e} \qquad (3.15a)$$

Where $$\left[B \right]^{e} = \left[\left[B \right]^{o}_{L}{}^{e} + \left[B \right]^{o}_{NL}{}^{e} \right] \qquad (3.15b)$$

The total mid plane strain is given by,

$$\left\{ \epsilon \right\}^{o} = \left[\left[B \right]^{o^{e}}_{L} + \frac{1}{2} \left[B \right]^{o^{e}}_{NL} \right] \left\{ \delta \right\}^{e} \qquad (3.16)$$

3.3.4 Expression for $d\left\{ \epsilon \right\}^{b}$ and $d\left\{ \epsilon \right\}^{s}$:

The bending and shear strain at the mid plane of the laminate can be written again in terms of nodal displacements as,

$$\left\{ \epsilon \right\}^{b} = \left[C \right]^{e} \left\{ \delta \right\}^{e}$$
$$\left\{ \epsilon \right\}^{s} = \left[D \right]^{e} \left\{ \delta \right\}^{e} \qquad (3.17a)$$

Where

$$[\,C\,]^e = [\,C_1,\ C_2\ ------\ C_9\,]$$
$$[\,D\,]^e = [\,D_1,\ D_2\ ------\ D_9\,] \qquad (3.17b)$$

and

$$[\,C_J\,] = \begin{bmatrix} 0 & 0 & 0 & \frac{\partial N_J^e}{\partial x_1} & 0 \\ 0 & 0 & 0 & 0 & \frac{\partial N_J^e}{\partial x_2} \\ C_o \frac{\partial N_J^e}{\partial x_2} & -C_o \frac{\partial N_J^e}{\partial x_1} & 0 & \frac{\partial N_j^e}{\partial x_2} & \frac{\partial N_J^e}{\partial x_1} \end{bmatrix} \qquad (3.17c)$$

$$[\,D_J\,] = \begin{bmatrix} 0 & -\frac{N_j^e}{R_2} & \frac{\partial N_j^e}{\partial x_2} & 0 & N_J^e \\ -\frac{N_j^e}{R_2} & 0 & \frac{\partial N_j^e}{\partial x_1} & N_J & 0 \end{bmatrix} \qquad (3.17d)$$

The first variation of bending strain and shear strain is given by,

$$d\{\in\}^b = [\,C\,]^e \{\,d\,\delta\,\}^e$$
and
$$d\{\in\}^s = [\,D\,]^e \{\,d\,\delta\,\}^e \qquad (3.18)$$

Substituting variation of strain relations (3.15a) and (3.18) in to virtual work equation (3.5) we get,

$$\bar{\psi}(\delta)= \int_A \left[\left\{ d\,\delta \right\}^{e^T} [\,B\,]^{e^T} \begin{Bmatrix} N_1 \\ N_2 \\ N_6 \end{Bmatrix} + \left\{ d\,\delta \right\}^{e^T} [\,C\,]^{e^T} \begin{Bmatrix} M_1 \\ M_2 \\ M_6 \end{Bmatrix} + \left\{ d\,\delta \right\}^{e^T} [\,D\,]^{e^T} \begin{Bmatrix} Q_1 \\ Q_2 \end{Bmatrix} \right] dx_1\, dx_2 - \left\{ d\delta \right\}^{e^T} \left\{ R \right\} = 0 \tag{3.19}$$

Where R contains nodal forces and is derived in next section. Eq. 3.19 can be written after taking out $\left\{d\delta\right\}^e$ as,

$$\psi(\delta)= \int_A \left[[\,B\,]^{e^T} \begin{Bmatrix} N_1 \\ N_2 \\ N_6 \end{Bmatrix} + [\,C\,]^{e^T} \begin{Bmatrix} M_1 \\ M_2 \\ M_6 \end{Bmatrix} + [\,D\,]^{e^T} \begin{Bmatrix} Q_1 \\ Q_2 \end{Bmatrix} \right] dx_1 dx_2 - \left\{ R \right\} = 0 \tag{3.20}$$

Eq. (3.20) represents a set of non linear equations to be solved for a bending problem.

3.3.5 Expressions For Stress Resultants :

The expressions for stress resultants N_1, N_2, N_6, M_1, M_2, M_6, Q_1 and Q_2 can be obtained by substituting the relations (3.16) and (3.17a) into Eq.(2.7) we get,

$$\left\{ N_1, N_2, N_6 \right\}^T = [\,QA\,]\,[\,B\,]_L^{o\,e}\left\{ \delta \right\}^e + \frac{1}{2}[\,QA\,]\,[\,B\,]_{NL}^{o\,e}\left\{ \delta \right\}^e + [\,QB\,]\,[\,C\,]^e\left\{ \delta \right\}^e \qquad (3.21a)$$

$$\left\{ M_1, M_2, M_6 \right\}^T = [\,QB\,]\,[\,B\,]_L^{o\,e}\left\{ \delta \right\}^e + \frac{1}{2}[\,QB\,]\,[\,B_{NL}^{o\,e}\,]\left\{ \delta \right\}^e + [\,QD\,]\,[\,C\,]^e\left\{ \delta \right\}^e \qquad (3.21b)$$

$$\left\{ Q_1, Q_2 \right\}^T = [\,QS\,]\,[\,D\,]^e\left\{ \delta \right\}^e \qquad (3.21c)$$

Substituting the expressions for stress resultants ie., relations (3.21a), (3.21b) and (3.21c) in (3.20) we obtain

$$\psi(\delta) = \int_A \Big[[\,B\,]_L^{o\,e^T}[\,QA\,][\,B\,]_L^{o\,e} + \frac{1}{2}[\,B\,]_L^{o\,e^T}[\,QA\,][\,B\,]_{NL}^{o\,e} + [\,B\,]_L^{o\,e^T}[\,QA\,][\,C\,]^e + [\,B\,]_{NL}^{o\,e^T}[\,QA\,][\,B\,]_L^{o\,e} + \frac{1}{2}[\,B\,]_{NL}^{o\,e^T}[\,QB\,][\,B\,]_{NL}^{o\,e} + [\,B\,]_{NL}^{o\,e^T}[\,QB\,][\,C\,]_L^{o\,e} + [\,C\,]^{e^T}[\,QB\,][\,B\,]_L^{o\,e} + \frac{1}{2}[\,C\,]^{e^T}[\,QB\,][\,B\,]_{NL}^{o\,e} + [\,C\,]^{e^T}[\,QD\,][\,C\,]^e + [\,D\,]^{e^T}[\,QS\,][\,D\,]^e \Big] \left\{ \delta \right\}^e dx_1 dx_2 - \left\{ R \right\} = 0 \qquad (3.22)$$

3.4 Solution of NonLinear Equilibrium Equations :

The nonlinear equilibrium equations can be solved by two different methods viz. the direct iteration method with incremental approach and the incremental newton-raphson method.

In the direct iteration method load is applied in small increments. Some initial solution is guessed (typically, $\delta = \{0\}$) and the equilibrium equations are solved to get new solution. This solution is used again to solve the equations. This type of iteration is continued till the two solutions converge. This method may not converge for highly nonlinear problems. Moreover it is computationally expensive.

In the Newton Raphson method to start with a solution is guessed. An improved solution ($\delta_i + d\delta_i$) is obtained from

$$\psi(\delta_i + d\delta_i) = \psi(\delta)\Big|_{\delta_i} + [K]_T \{ d\delta \} = 0 \qquad (3.23a)$$

where K_T is the tangent stiffness matrix given by,

$$[K]_T = \left[\frac{\partial \psi(\delta_i^e)}{\partial (\delta)^e} \right] \qquad (3.23b)$$

Eqn. (3.23a) gives nonlinear incremental equilibrium equations which gives the linearized approximation to the relation between residual forces and the incremental displacements.

The new improved solution can be found as

$$\delta_{i+1} = \delta_i + d\,\delta_i \qquad (3.24)$$

To improve numerical stability the load $\{R\}$ is applied in small increments.

3.5 Tangent Stiffness Matrix :

The tangent stiffness matrix for a element can be written as,

$$[K]_T = \begin{bmatrix} \frac{\partial \psi_1}{\partial \delta_1} & \frac{\partial \psi_1}{\partial \delta_2} & \cdots & \frac{\partial \psi_1}{\partial \delta_N} \\ \frac{\partial \psi_2}{\partial \delta_1} & \frac{\partial \psi_2}{\partial \delta_2} & \cdots & \frac{\partial \psi_2}{\partial \delta_N} \\ . & . & & . \\ \frac{\partial \psi_N}{\partial \delta_1} & \frac{\partial \psi_N}{\partial \delta_2} & \cdots & \frac{\partial \psi_N}{\partial \delta_N} \end{bmatrix} \qquad (3.25)$$

Where N is the total degree of freedom of the element.

An element $K_{Ti,j}$ in Eq.(3.20) can be written as

$$K_{Ti,j} = \frac{\partial \psi_i}{\partial \delta_j} = \int_A \left[\sum_{k=1}^{3} \left[B_{ki} \frac{\partial N_k}{\partial \delta_j} + N_k \frac{\partial B_{ki}}{\partial \delta_j} + C_{ki} \frac{\partial M_k}{\partial \delta_j} \right] + \sum_{k=1}^{2} D_{ki} \frac{\partial Q_k}{\partial \delta_j} \right] dx_1 dx_2 \qquad (3.26)$$

Where $\dfrac{\partial R}{\partial \delta_j} = 0$

It is shown in the Appendix – II that the tangent stiffness matrix can be written as

$$[K]_T = \int \left[[B]^{e^T} [QA] [B]^e + [B]^{e^T} [QB] [C]^e + [C]^{e^T} [QB] [B]^e + [C]^{e^T} [QD] [C]^e + [D]^{e^T} [QS] [D]^e + [G]^{e^T} \begin{bmatrix} N_1 & N_6 \\ N_6 & N_2 \end{bmatrix} [G]^e \right] dx_1 dx_2 \qquad (3.27)$$

Using the relations (3.15b) in Eqn. (3.27) the tangent stiffness matrix can be written as

$$[K]_T = [K]_L + [K]_{NL} + [K]_\sigma \qquad (3.28a)$$

Where

K_L Linear stiffness matrix

K_{NL} Initial displacement matrix

K_σ Initial stress matrix

$$[K]_L = \int_A \Big[[B]_L^{o\,e^T} [QA] [B]_L^{o\,e} + [B]_L^{o\,e^T} [QB] [C]^e + [C]^{e^T} [QB] [B]_L^{o\,e} + [C]^{e^T} [QD] [C]^e + [D]^{e^T} [QS] [D]^e \Big] dx_1\, dx_2 \qquad (3.28b)$$

$$[K]_{NL} = \int_A \Big[[B]_L^{o\,e^T} [QA] [B]_{NL}^{o\,e} + [B]_{NL}^{o\,e^T} [QA] [B]_L^{o\,e} + [C]^{e^T} [QB] [B]_{NL}^{o\,e} + [B]_{NL}^{o\,e^T} [QB] [C]^e + [B]_{NL}^{o\,e^T} [QA] [B]_{NL}^{o\,e} \Big] dx_1\, dx_2 \qquad (3.28c)$$

$$[K]_\sigma = \int_A [G]^{e^T} \begin{bmatrix} N_1 & N_6 \\ N_6 & N_2 \end{bmatrix} [G]^e \, dx_1\, dx_2 \qquad (3.28d)$$

3.6 Elemental Force Vector :

The work done by external loads for the bending problem may be independent or combination of these load cases.

(i) Concentrated loads R_c acting in the direction of the

corresponding nodal degree of freedom.

(ii) Uniformly distributed load on the surface.

The total external work done by these forces on an element can be written as

$$W_{ER}^{e} = \left\{\delta\right\}^{e^T}\left[\left\{R_c\right\} + \int_A \left\{S\right\}^{e^T} R_o \, dA\right]$$

$$W_{ER}^{e} = \left\{\delta\right\}^{e^T}\left\{R\right\}^{e} \qquad (3.29)$$

R_c is vector containing nodal forces/couples at node J in the direction of that nodal degree of freedom. The vector R_o can be written as

$$\left\{R_o\right\}^T = \left\{R_{01}, R_{02}, - - - - - - R_{09}\right\}^T \qquad (3.30)$$

and R_{oJ} is given by $\left\{\begin{array}{ccccc} 0 & 0 & \bar{R}_o & 0 & 0 \end{array}\right\}$

$$\left\{S\right\}^e = \left\{S_1, S_2, - - - - - - S_9\right\}^T \qquad (3.31)$$

each S_J is given by $\left\{\begin{array}{ccccc} 0 & 0 & N_J & 0 & 0 \end{array}\right\}$

3.7 Geometric Stiffness Matrix for the Plate Problem :

For the linear buckling problem the geometric stiffness matrix can be derived by considering the work done by in plane

forces N_1, $N_2$and N_6 at the mid plane of the laminate. The datum configuration is taken as initially compressed configuration. The mid plane strains due to bending can be written as

$$\epsilon_1 = \frac{1}{2}\left(\frac{\partial u_3}{\partial x_1}\right)^2$$

$$\epsilon_2 = \frac{1}{2}\left(\frac{\partial u_3}{\partial x_2}\right)^2 \qquad (3.32)$$

$$\epsilon_6 = \left(\frac{\partial u_3}{\partial x_1}\right)\left(\frac{\partial u_3}{\partial x_2}\right)$$

The work done by these forces is given by

$$W_{EG}^{e} = \frac{1}{2}\int_A N_1\left(\frac{\partial u_3}{\partial x_1}\right)^2 + N_2\left(\frac{\partial u_3}{\partial x_2}\right)^2 + 2N_6\left(\frac{\partial u_3}{\partial x_1}\right)\left(\frac{\partial u_3}{\partial x_2}\right) dx_1 dx_2 \qquad (3.33)$$

Eqn. (3.33) can be written as

$$W_E^{e} = \frac{1}{2}\int \left\{\begin{matrix}\frac{\partial u_3}{\partial x_1}\\ \frac{\partial u_3}{\partial x_2}\end{matrix}\right\}^T \begin{bmatrix} N_1 & N_6 \\ N_6 & N_2 \end{bmatrix} \left\{\begin{matrix}\frac{\partial u_3}{\partial x_1}\\ \frac{\partial u_3}{\partial x_2}\end{matrix}\right\} dx_1\, dx_2 \qquad (3.34)$$

Expressing the terms $\frac{\partial u_3}{\partial x_1}$ and $\frac{\partial u_3}{\partial x_1}$ in terms of shape functions and nodal displacements Eqn. (3.34) can be rewritten as

$$W_E^e = \int_A \left[\frac{1}{2} \right] [\delta]^{e^T} [G]^{e^T} \begin{bmatrix} N_1 & N_6 \\ N_6 & N_2 \end{bmatrix} [G]^e [\delta]^e dx_1 dx_2 \qquad (3.35)$$

In this expression ,the stress resultants N_1, N_2 and N_6 are constant over the domain and will be equal to applied forces. The in plane forces N_1, $N_2$and N_6 can be expressed as

$$N_1 = \lambda\, n_1 \; ; \quad N_2 = \lambda\, n_2 \; ; \quad N_6 = \lambda\, n_6 \qquad (3.36)$$

Substituting the relation (3.36) in (3.35) and rewriting the expression for external work we obtain

$$W^e = \frac{1}{2} \lambda [\delta]^{e^T} [K]_G [\delta]^e \qquad (3.37)$$

Where K_G is the geometric stiffness matrix

The first variation of the work done by external in plane forces can be written by considering the symmetry of K_G as,

$$dW_E^e = \lambda [d\delta]^{e^T} [K]_G^e [\delta]^e \qquad (3.38)$$

Now the equilibrium equations for a linear buckling problem can be written as,

$$[d\delta]^e [K]_L^e [\delta]^e - \lambda [d\delta]^e [K]_G^e [\delta]^e = 0 \qquad (3.39)$$

or $$\left[[K]_L^e - \lambda [K]_G^e \right][\delta]^e = 0 \qquad (3.40)$$

Eqn. (3.40) represents typical eigen value problem. On solving, the lowest magnitude of eigen value gives the buckling load. The eigen vector represents the mode shape.

3.8 Geometric Stiffness Matrix for the Shell Problem :

The geometric stiffness matrix or the shell problem can be derived by considering the work due to pre buckling stresses (N_1, N_2, and N_δ) during the buckling.

The work done expression can be written as

$$W_E^e = \frac{1}{2} \int N_1 \left[\left(\frac{\partial u_1}{\partial x_1}\right)^2 + \left(\frac{\partial u_2}{\partial x_1}\right)^2 + \left(\frac{\partial u_3}{\partial x_1}\right)^2 \right] + N_2 \left[\left(\frac{\partial u_1}{\partial x_2}\right)^2 + \left(\frac{\partial u_2}{\partial x_2}\right)^2 + \left(\frac{\partial u_3}{\partial x_2}\right)^2 \right] + 2N_\delta \left[\left(\frac{\partial u_1}{\partial x_1}\right)\left(\frac{\partial u_1}{\partial x_2}\right) + \left(\frac{\partial u_2}{\partial x_1}\right)\left(\frac{\partial u_2}{\partial x_2}\right) + \left(\frac{\partial u_3}{\partial x_1}\right)\left(\frac{\partial u_3}{\partial x_2}\right) \right] dx_1 dx_2 \qquad (3.41)$$

Expressing u_1, u_2 and u_3 in terms of shape functions and the total expression will become similarly as Eqn.(3.37).This K_G matrix is substituted in equilibrium equations and solved for the eigen value problem. The lowest eigen value is the buckling load.

The integrals involved in the expressions of $\psi(\delta)$, K_L, K_{NL} and K_σ are evaluated using gauss - quardrature. The exact

integration of the stiffness matrix requires 3x3 gauss point rule. But, at the thin plate limit to overcome locking 2x2 gauss quadrature is used for shear energy terms, while 3x3 is used for non shear terms. In the above section equilibrium equations are developed for an element. These equations can be assembled using the connectivity at the element interface. Proper boundary conditions are applied and the assembled equations are solved.

CHAPTER 4

RESULTS AND DISCUSSION

4.1 Introduction :

The equations developed in Chapter 3 are employed for numerical studies on some typical plates and shells. The results obtained (ie.,present linear theory (PLT), present nonlinear theory (PNLT)), are compared with some experimental, higher order theories (HSDT) and classical plate theory (CPT) results. Results are presented in the form of graphs and tables. The parameter whose effect is examined include number of layers, side to thickness ratio (radius to thickness ratio for shell) and orthotropy. The effect of different simply-supported boundary conditions on bending-stretching coupling is also investigated.

The finite element used for the discretization of plates and shells is a nine noded shell element. In the present work a shear correction factor (5/6) has been used. Reduced integration has been used for transverse terms in the case of thin plates and shells because full integration leads to over stiff results. The plate problems are solved by taking the radius of curvature very large (typically 10^{30}) in strain displacement relations Eqn. (2.3a) The boundary conditions used in the present work are shown in the Fig. 2.3.

For linear problems the matrices K_L and K_σ, in formulating tangent stiffness matrix are put as zero. For stability problems the matrix K_G matrix is formed and Eqn. (3.40) is solved for the eigen value.

For nonlinear bending problems a solution $\delta = \left\{ 0 \right\}$ is assumed and for the first iteration linear solution is obtained. Using the linear solution the matrices K_{NL} and K_σ are computed and solution is found again from the Newton - Raphson iteration. The iterations are continued till the two successive solutions δ^i, δ^{i+1} converge. The following convergence criterion is used.

$$\frac{\delta_k^{\,i+1} - \delta_k^{\,i}}{\left| \delta_k^{\,i} \right|} < 1 \times 10^{-3}$$

Where i is the iteration counter and k is the nodal variable counter.

Whenever symmetry exists quarter plate model has been employed. Unless specified, a 3X3 mesh is used for bending and a 2X2 is used for buckling problems. The following nondimensional deflections and buckling loads are used.

$$\bar{u}_3 = \frac{u_3 E_2 h^3}{R_o a^4}$$

$$\bar{N}_x = \frac{N_x b^2}{E_2 h^3}$$

Where u_3 is calculated at the center of the plate. N_x is the applied critical load in case of linear buckling problem.

4.2 Presentation of Results and Discussion :

The following types of problems are solved using the formulation given in chapter 3.

4.2.1 Bending Analysis

(a) Numerical accuracy of the present model with respect to the element

(b) Bending analysis of three layered cross-ply

(c) Bending analysis of angle-ply

(d) A comment on the boundary conditions

(e) Bending of isotropic spherical shell

(f) Bending of cylindrical shell

(g) Cross-ply freely supported cylindrical shell under sinusoidal load

4.2.2 Stability Analysis

(a) Stability of isotropic plate

(b) Stability of symmetric cross-ply

(c) Stability of angle-ply

(d) Stability of isotropic cylindrical shell

4.2.3 Nonlinear Bending Analysis of Plates

(a) Nonlinear analysis of orthotropic plate

(b) Nonlinear analysis of symmetric cross-ply

(c) Nonlinear analysis of simply supported cross-ply and angle-ply

(d) Nonlinear analysis of clamped corss-ply and angle-ply

(e) Sandwich plates

4.2.4 Post Buckling of Isotropic Plate

4.2.1a Numerical Accuracy of the Present Model with respect to the Element :

To check the numerical accuracy of the present element a test problem is solved for which closed form solution (CFS) is available [11].

A simply supported square cross-ply (0/90/90/0) laminate with the following properties was considered under sinusoidal loading.

$$\frac{E_1}{E_2} = 25 \qquad \frac{G_{12}}{E_2} = 0.5 \qquad \frac{G_{23}}{E_2} = 0.2 ,$$

$$\nu_{12} = 0.25 \qquad G_{12} = G_{13} \tag{4.1}$$

The results of non dimensionalized deflections $\bar{u}_3$ were obtained for the following cases

(a) Full integration (3X3 gauss rule for bending terms and 3X3 gauss rule for shear terms)

(b) Mixed integration (3X3 gauss rule for bending terms and 2X2 gauss rule for shear terms)

(c) Reduced integration (2X2 gauss rule for bending and shear terms)

The solutions were obtained using s1 boundary conditions

which are used in Ref [11] for the quarter plate model.

The results for various thickness ratios were obtained and presented in table 4.1. We can conclude from the results that

(1) The nine noded element give virtually same results for full, mixed and reduced integration schemes.

(2) As thickness of the plate is reducing it can be seen that full integration gives over stiff results. This is due to the reason that the present model being not able to satisfy the Kirchoff's condition as a constraint. It can also be seen that the results with mixed integration scheme exactly agree with closed form solutions. No significant difference is observed between reduced integration and closed form solutions. However the experience of the people in this field says that mixed integration is suitable for thin plate or thin shell situations. Therefore we used reduced integration for the shear terms in these cases.

(3) The finite element model used here is expected to yield correct results.

4.2.1b Bending analysis of Three Layered Cross-Ply :

The object of this study is to compare the present theory with the closed form solutions of higher order shear deformation theory (HSDT) presented by Reddy [16]. The higher order theories are computationally expensive and involve large number of degrees of freedom.

A simply supported three layered corss-ply (0/90/0) of the following material properties subjected to uniformly distributed

lateral load is taken up for which HSDT results are available

$$E_1 = 19.2 \times 10^6 \text{ psi}, \qquad E_2 = 1.56 \times 10^6 \text{ psi},$$
$$G_{12} = G_{13} = 0.82 \times 10^6 \text{psi}, \qquad G_{23} = 0.523 \times 10^6 \text{psi},$$
$$\nu_{12} = 0.24 , \quad a = b = 10 \text{ in.} \qquad (4.2)$$

The results are obtained using s1 boundry conditions. The non dimensionalized deflections $\bar{u}_3$ are presented for various thickness ratios in table 4.2.

It can be seen from the results presented in table 4.2 that the present results are close to the HSDT results for a/h >10 without much computational effort. The maximum difference is about 2.7%. The present results underestimate the deflections compared to HSDT. It can be seen that the difference reduces as the thickness of the plate decreases. The CPT results underestimate the deflections and are not reliable at thick plate limit. It can be concluded that present theory is adequate in predicting the deflections for a/h > 10

4.2.1c Bending Analysis of Angle-Ply :

In this section the effect of bending-stretching coupling on linear deflections for an angle-ply (-45/45/...) is studied. A simply supported angle-ply made of graphite epoxy of the following material and geometrical properties subjected to uniformly distributed lateral load is taken up.

$$\frac{E_1}{E_2} = 40, \quad G_{23} = 0.5\ E_2, \quad G_{12} = G_{13}\ 0.6\ E_2,$$
$$\nu_{12} = 0.25, \quad E_2 = 10^6 \text{ psi}$$
$$a = b = 10 \text{ in.} \tag{4.3}$$

Fig. 4.1 shows the plot of nondimensionalized central deflections for various thickness ratios with increasing number of layers. The results are obtained using s2 boundary conditions in a quarter plate. It can be seen that the deflections for two layers are higher than the four layer and eight layers. This is due to the bending stretching coupling which is maximum for two layers and decreases as the number of layers is increased.

4.2.1d A Comment on the Boundary Conditions :

To study the effect of different in plane boundary conditions on bending–stretching problems a two layer angle-ply and cross-ply of the material properties given in Eqn. (4.3) subjected to uniformly distributed lateral load is taken.

$$a = b = 10 \text{ in. } h = 0.1 \text{ in.} \tag{4.4}$$

One can use s1 boundary conditions and s2 boundary conditions as a symmetry conditions for the quarter plate model associated with cross-ply and angle-ply respectively. However one cannot use the symmetry conditions s1 in the quarter model of angle-ply and s2 in the quarter plate model of cross-ply. The effect of different boundary conditions on the linear bending of

$$\frac{E_1}{E_2} = 40, \quad G_{23} = 0.5\, E_2, \quad G_{12} = G_{13}\, 0.6\, E_2,$$
$$\nu_{12} = 0.25, \quad E_2 = 10^6 \text{ psi}$$
$$a = b = 10 \text{ in.} \tag{4.3}$$

Fig. 4.1 shows the plot of nondimensionalized central deflections for various thickness ratios with increasing number of layers. The results are obtained using s2 boundary conditions in a quarter plate. It can be seen that the deflections for two layers are higher than the four layer and eight layers. This is due to the bending stretching coupling which is maximum for two layers and decreases as the number of layers is increased.

4.2.1d A Comment on the Boundary Conditions :

To study the effect of different in plane boundary conditions on bending–stretching problems a two layer angle–ply and cross–ply of the material properties given in Eqn. (4.3) subjected to uniformly distributed lateral load is taken.

$$a = b = 10 \text{ in. } h = 0.1 \text{ in.} \tag{4.4}$$

One can use s1 boundary conditions and s2 boundary conditions as a symmetry conditions for the quarter plate model associated with cross–ply and angle–ply respectively. However one cannot use the symmetry conditions s1 in the quarter model of angle–ply and s2 in the quarter plate model of cross–ply. The effect of different boundary conditions on the linear bending of

cross-ply and angle-ply are showed in the table 4.3. It can be seen that for N = 2 layers, the difference between the deflections obtained from these boundary conditions (S1 and S2) is maximum. But for N = 10 the difference is small. This due to the fact that as the number of layers are increased the bending-stretching coupling decreases and the effect of different in plane boundary conditions is not significant.

4.2.1e Bending of Isotropic Spherical Shell :

A simply supported isotropic spherical shell shown in Fig.(4.2a) of the following material and geometrical properties is studied under a concentrated load of 100 lbs.

$$E = 10^7 \text{ psi}, \quad \nu = 0.3, \quad h = 0.1 \text{ in.} \quad R_1 = R_2 = 96 \text{ in.}$$
$$a = b = 32 \text{ in.} \qquad (4.5)$$

Due to the existence of the symmetry a 2X2 mesh is used to discretise one quadrant of the shell. As the shell is thin (R/h = 320), mixed integration is used. The linear deflection obtained under the concentrated load is 0.03723 in. The mesh is refined to 3X3 and the central deflection obtained is 0.03886 in. in comparison to 0.038661 in. of Rao [37] whose result is based on classical shell theory where shear deformation is neglected.

4.2.1f Bending of Cylindrical Shell :

A clamped isotrpic cylindrical shell shown in Fig. (4.2b)

of the following material and geometric properties subjected to uniformly distributed lateral load is considered for the study.

$$E = 3103 \ N/mm^2, \quad \nu = 0.3, \quad h = 3.175, \quad a = 254 \ mm.$$
$$R_o = 1000 \times 10^{-6} \ N/mm^2 \quad \theta = 0.1 \ rad. \qquad (4.6)$$

Here a 3X3 mesh is used to descretize one quadrant of the shell. Clamped boundary conditions given in Eqn. (2.10) are used. The linear central deflection obtained at the center of the shell is 0.84297 in. compared to 0.8250 in. of Dutt whose result is based on classical shell theory. The Dutt result was given in Ref.[39]

4.2.1g Cross-ply Freely supported Cylindrical Shell under Sinusoidal Load :

A cylindrical cross-ply (0/90/90/0) cylindrical shell of the material properties given in Eqn (4.1) subjected to sinusoidal loading is taken for the study. The geometrical properties are

$$a/b = 1.0, \quad a/h = 10 \quad R_2 = 10^{30}$$
$$R_o = \bar{R}_o \ SIN \frac{\pi x_1}{a} \ SIN \frac{\pi x_2}{b} \qquad (4.7)$$

The following boundary conditions are imposed

$$u_3 = u_2 = 0 \quad \text{at} \quad x_1 = 0,a$$
$$u_3 = u_1 = 0 \quad \text{at} \quad x_2 = 0,b \qquad (4.8)$$

For this special case of boundary conditions , loading closed form solutions are available in Ref [38] with the same theory. A 4x4 element mesh is used to descretize the quarter shell. The nondimensional deflections $\bar{u}_3$ are presented in Table 4.4 for a/h = 10 and a/h =100. It can be seen that the FEM results are close to the closed form solutions.

4.2.2 Stability Analysis :

In this section stability of isotropic plates and cross-ply plates have been compared with HSDT results. Bending stretching coupling on angle-ply laminates has been studied. Results are presented for cylindrical shell under axial compressive load.

4.2.2a Stability of Isotropic Plates :

The object of this study is to evaluate higher order theories with respect to their computational power and accuracy. A simply supported isotropic square plate of the following material and geometric properties under uniaxial compressive load is considered.

$$E = 10^7 \text{psi}, \quad \nu = 0.3, \quad a = b = 10 \text{ in.} \qquad (4.9)$$

A 2X2 mesh is used to discretize the quadrant of the plate. s1 boundary conditions are used and linear buckling load is

computed by solving the eigen value problem. Nondimensional buckling loads are presented in table 4.5 and compared with closed form solutions of HSDT by Reddy [17] for various thickness ratios. It can be seen from the results the present results are very close to HSDT results for all thickness ratios. The maximum difference is 0.75%. The difference is decreasing as the thickness is decreasing. But in the results shown this effect cannot be seen over the whole range due to the small error in the eigen value calculation of large matrices and locking phenomenon. The CPT results over estimate the buckling loads for thick plates (a/h < 20). This due to the shear deformation neglected in CPT.

4.2.2b Stability of Symmetric Cross-Ply :

A simply supported graphite epoxy symmetric cross-ply (0/90/90/0) laminate of the material properties given in Eqn. (4.3) is considered to study the uniaxial buckling load.

The nondimensional uniaxial buckling load $\bar{N}_x$ was computed and presented in table 4.6 with HSDT results [17]. s1 boundary conditions are used.

It can also seen from the results that the present results are very close to HSDT results. The maximum difference is 1.5%. It implies the adequacy of the present theory in predicting the buckling loads. HSDT in FEM will involve a lot of additional computational effort without improvement in the results. From Table 4.5 and 4.6 we can conclude that the difference between the present theory and the HSDT is slightly increasing with the

orthotropy.

4.2.2.c Stability of Angle-Ply :

A simply supported square angle-ply (45/-45/...) under uniaxial compression load is considered for the study. The properties of individual laminate are given in Eqn. (4.3).

Solutions are obtained for S2 boundary conditions in a quarter plate. Fig. 4.3 displays the variation of nondimensional buckling load $\bar{N}_x$ with fibre orientation and number of layers. It is shown [41] that the solution approaches to orthotropic solution at N = 6. Hence in the present study N = 6 and N = 2 are considered for a/h = 10 and a/h = 100. It can be seen that as the number plates increased the buckling load is increasing for the same thickness. This is due to the reduction in the bending stretching coupling and buckling load is minimum for two layer laminates. There is significant difference between the results for a/h = 10 and a/h = 100. This is due to shear deformation which decreases the buckling load. At 45^0 orientation the buckling loads are maximum for all number of layers.

4.2.2.d Buckling of Isotropic Cylindrical Shell under Axial Load :

An isotropic homogeneous cylindrical shell with length 11 in.,radius of 36 in., and thickness of 0.125 in. is considered as a test problem to check the formulation. Both the edges are simply supported. The analytical solution for the same is available with

Donnell's theory in Ref [42]. For the finite element modeling it is assumed that symmetric conditions prevails at the mid length and that the cylinder buckles in 15 circumferencial full waves as shown in the Fig. (4.4a). Consequently a 5.5 in. long and 12^{o} wide cylindrical segment is considered with symmetrical conditions imposed on the three sides. The following boundary conditions are used

$$\begin{aligned} u_2 = u_3 = \phi_2 = 0 \quad & \text{on} \quad x_1 = 0,a \\ u_1 = u_3 = \phi_1 = 0 \quad & \text{on} \quad x_2 = 0 \\ u_2 = \phi_2 = 0 \quad & \text{on} \quad x_2 = b \end{aligned} \tag{4.10}$$

where coordinate axes pass through left corner of the segment as shown in the Fig (4.4b).

The eigen value problem of Eqn. (3.42) is solved and buckling load is applied as 2721 lb/in. The result is with a difference of 3.5% with the analytical solution (2625 lb/in.) given in Ref.[42]. This difference is likely to get reduced as the mesh is refined. This is being the reason that as the shell is very thin and the shear deformation effect is expected to be negligible and the results obtained from the present theory can be compared with the Donnell's theory given in Ref. [42] which does not take into shear deformation.

In the present study we could not make use of a routine SSPACE given in Ref. [43] which computes specified number of lowest eigen values only. Hence we could not go in for a refined mesh than 2X2 because of the computational limitation. Laminated shells buckles in more than one half wave along the axial

was obtained by using both Newton- Raphson and picard iteration. Table 4.7 shows the results obtained from Newton-Raphson and picard type of iteration.

It is evident from Table 4.7 that the number of iterations for convergence increases with the load when picard iteration is used. However Newton-Raphson converges in three iterations for all loads. Hence in the problems investigated below Newton-Raphson method has been employed.

A 2X2 mesh is used in quarter plate. Using Newton-Raphson results were obtained with S1 and S3 boundary conditions. Fig. (4.5) displays the results obtained from present linear results (PLT), present nonlinear results (PNLT), classical linear results (CLT) and classical nonlinear results (CNLT) given in Ref. [18]. It can be seen that the PLT and CLT results are close. This is due to the fact that as the plate is very thin (a/h = 87) the effect of shear deformation is expected to be negligible. It can be seen that compared to CNLT results the PNLT results obtained with S1 boundary conditions are in close agreement with the experimental results. This is due to the reason that the boundary conditions used in Ref. [18] to obtain the CNLT solution are $u_1 = u_2 = u_3 = 0$ and $M_2 = 0$ at the simply supported edge which may not correspond to the the experimental conditions. The PNLT results obtained with S3 boundary conditions are away from the experimental results. The difference between S1 and S3 boundary conditions are due to the bending stretching introduced through the nonlinear term.

It can be concluded that the practical simply-supported

boundary conditions for the orthotropic plate can be in between S1 and S3 boundary conditions.

4.2.3b Nonlinear analysis of Cross-Ply :

A clamped symmetric cross-ply (0/90/90/0) of the following material and geometric properties used to study the nonlinear analysis under uniformly distributed load. For this data CLT, CNLT and experimental results are avalible in [18].

$$a = b = 12 \text{ in.} \quad h = 0.096 \text{ in.}$$
$$E_1 = 1{,}828 \times 10^6 \quad , \quad E_2 = 1.8315 \times 10^6$$
$$G_{12} = G_{13} = G_{23} = 3.125 \times 10^6$$
$$\nu_{12} = \nu_{13} = \nu_{23} = .2395 \qquad (4.12)$$

The CPT, CNLT, PLT, PNLT and experimental results are presented in Fig. (4.6) with load intensity. In this case there is a difference between CLT and PLT reults even though the plate is thin. This is because in the Ref. [18] the following boundary conditions are used at the clamped edge in the linear and nonlinear analysis

$$u_1 = u_2 = u_3 = \frac{\partial u_3}{\partial x_2} = 0 \qquad (4.13)$$

which over estimates the deflections. But in the present FEM model it is possible to specify the correct boundary conditions which are given in Eqn.(2.10). The PNLT results are lower than the experimental results which shows the correct trend. The reason of

difference in the results is that the clamped boundary conditions are not satisfactorily imposed during the experimentation as stated in the Ref.[18]. The CNLT results shows altogether different trend because of the reason mentioned above regarding boundary conditions. These two examples led to the confidence in the present model in predicting the accurate nonlinear response of the composite plates.

4.2.3c Nonlinear Analysis of Simply Supported Cross-Ply and Angle-Ply :

A simply supported square plate of the following material properties is taken for the study.

$$\frac{E_1}{E_2} = 24 \quad , E_2 = 7.031 \times 10^5 \ N/cm^2 \ , \quad \frac{G_{12}}{E_2} = .5$$

$$G_{13} = G_{12} \quad , \quad \frac{G_{23}}{E_2} = .2 \quad , \quad \nu_{12} = .25$$

$$a = b = 243.8 \text{ cm.} \qquad h = .635 \qquad (4.15)$$

As the bending-stretching coupling is maximum for two layer laminates a two layer angle-ply and cross-ply subjected to uniformly distributed lateral load is considered. The load deflections curves are shown in Fig. (4.7) and Fig. (4.8). For the cross-ply S1 and S3 boundary conditions are used.It can be seen that S3 boundary conditions are stiffening type than S1 boundary conditions. The same trend is shown for the orthotropic plate in Fig. (4.4). For the angle-ply S2 and S3 boundary conditions are

used. Here also S3 boundary conditions show the same trend with S2 boundary condition.

4.4.3d Nonlinear Analysis of Clamped Cross-ply and Angle-Ply :

A clamped cross-ply and angle-ply of the material properties shown in Eqn.(4.3) is used to study the nonlinear behavior.

Fig. (4.9) and Fig.(4.10) shows the load deflection curves for two layer cross-ply and angle-ply. It can be seen that the two layer cross-ply exhibits more nonlinearity than angle-ply. It can also seen that for cross-ply as the number of layers are increased from two layers to eight layers the nonlinearity is decreasing. This is due to the reduction in bending-stretching coupling with the number of layers.

4.2.3e Sandwich Plates :

The object of this study is to validate the present theory to sandwich plates by comparing with the available experimental results. A simply supported square sandwich laminate with aluminium faces and balsa core subjected to uniform transverse pressure is studied with the following face properties.

$$E_f = 10 \times 10^6, \qquad t_f = 0.32 \text{ in.}$$

A 2x2 mesh is used to idealize one quarter plate and S3 boundary condition are used. The results are obtained from the present theory and experimental results are presented in Table 4.8

and table 4.9 for varying spans, core thickness, core shear rigidity and load intensities. The present nonlinear results compare satisfactorily with the experimental results. When the shear rigidity of the core high it can be concluded that neglecting the face shear rigidity yields better results than considering the shear rigidity of the face plate.

4.2.4 Post buckling of Isotropic Plate :

A simply supported isotropic square plate of the following material properties is chosen for the study

$$E = 30 \times 10^{6} \text{Psi}, \quad a = b = 10 \text{ in.} \quad h = 0.1 \text{ in.}$$

In this problem following type of boundary conditions were used

$$\begin{aligned} u_1 &= C_1 \text{ SIN } \frac{\pi x_1}{a} \text{ COS } \frac{\pi x_2}{2b} \\ u_2 &= C_2 \text{ COS } \frac{\pi x_1}{2a} \text{ SIN } \frac{\pi x_2}{b} - \epsilon x_2 \\ u_3 &= C_3 \text{ COS } \frac{\pi x_1}{2a} \text{ COS } \frac{\pi x_2}{2b} \end{aligned} \qquad (4.16)$$

Here the origin is chosen at the centre of the plate. 2a and 2b are the dimensions of the plate respectively.

The boundary conditions can be rewritten as

$$\begin{aligned} u_1 = u_3 &= 0 && \text{on all edges,} \\ u_2 &= -\epsilon x_2 && \text{on } x_1 = \pm a \\ u_2 &= \pm \epsilon b && \text{on } x_2 = \mp b \end{aligned} \qquad (4.17)$$

After the application of these boundary conditions the problem becomes the minimization of strain energy as the variation of potential energy is zero.

From Ref. [42] the critical value of ϵ where a buckled configuration exists for $\nu = 0.3$ is

$$\epsilon_{cr} = 0.632 \frac{h^2}{a^2} \qquad (4.18)$$

ie., if $\epsilon < \epsilon_{cr}$ the plate will be in compressed configuration only

Let $$n = \frac{\epsilon}{\epsilon_{cr}}$$

A small lateral load 2lbs (0.18% of the critical load) is applied at the centre of the plate to initiate buckling. The buckled configuration serves as starting vector for the iteration.

The central deflection computed for various values of n iteratively are presented with analytical Gelerkian solution obtained in Ref. [42] in Fig. 4.11. It can be seen that the present FEM results and Gelerkian solution are agreeing.

Table 4.1 Nondimensionalized centre deflections of cross-ply (0/90/90/0) under sinusoidal loading.

a/h	CFS	Full	Mixed	Reduced
10	6.627	6.617	6.625	6.623
20	4.911	4.887	4.912	4.908
100	4.337	4.190	4.336	4.333

Table 4.2 Nondimensionalized centre deflections of three layered cross-ply (0/90/0) under uniformly distributed load.

a/h	HSDT	Present	CPT
2	7.258	7.062 (2.70)	1.206
5	2.324	2.275 (2.13)	1.206
10	1.510	1.485 (1.63)	1.206
20	1.280	1.274 (0.45)	1.206

Table 4.3 Nondimensionalized center deflections of cross-ply and angle-ply with different boundary conditions

		cross-ply		Angle-ply	
N	$\frac{x}{a}$	S1*	S2	S2*	S1
2	0.000	1.4048	1.1539	0.8923	0.4804
	0.125	1.3050	1.0731	0.8336	0.7335
	0.250	1.0180	0.8321	0.8591	0.5843
	0.375	0.5652	0.4580	0.3726	0.3317
	0.500	0.0000	0.0000	0.0000	0.0000
10	0.000	0.6190	0.6170	0.4013	0.4007
	0.125	0.5771	0.5753	0.3766	0.3761
	0.250	0.4543	0.4530	0.3017	0.3013
	0.375	0.2565	0.2551	0.1746	0.1743
	0.500	0.0000	0.0000	0.0000	0.0000

* Correct boundary conditions to be used in the quarter plate model

Table 4.4 Nondimentionalized centre deflections of cross-ply (0/90/90/0), freely supported cylindrical shell under sinusoidal loading

R/h	Present FEM	CFS
100	0.6590	0.6610
10	0.5188	0.5254

Table 4.5 Nondimensionalized buckling loads $\bar{N}_x$ for isotropic square plates

a/h	HSDT	Present	CPT
10	3.7865	3.8151 (0.754)	4.000
20	3.9443	3.9476 (0.083)	4.000
50	3.9909	3.9943 (0,085)	4.000
100	3.9977	4.0012 (0.970)	4.000

Table 4.6 Nondimensionalized deflections for symmetric cross-ply (0/90/90/0)

a/h	HSDT	Present	CPT
5.0	11.008	10.9916 (0.149)	35.831
10.0	22.160	22.3531 (0.864)	35.831
12.5	25.590	25.854 (1.039)	35.831
20.0	30.922	31.3340 (1.332)	35.831
25.0	32.515	33.0000 (1.49)	35.831
50.0	34.936	35.2800 (0.985)	35.831
100.0	35.602	35.9600 (1.00)	35.831

Table 4.7 Results obtained for Newton-Raphson and and Picard Iteration for the Orthotropic Plate

Load	No. of iterations	Picard	Newton-Raphson
0.2	1	4.5365 E-02	4.5365 E-02
	2	4.3818 E-02	4.4142 E-02
	3	4.3928 E-02	4.3917 E-02
	4		4.3928 E-02
0.4	1	8.7836 E-02	8.5241 E-02
	2	8.0171 E-02	8.2001 E-02
	3	8.1796 E-02	8.1515 E-02
	4	8.1467 E-02	8.1522 E-02
	5	8.1578 E-02	8.1522 E-02
0.6	1	0.1223	0.1154
	2	0.1085	0.1125
	3	0.1135	0.1122
	4	0.1117	
	5	0.1123	
	6	0.1121	
0.8	1	0.1497	0.1399
	2	0.1316	0.1377
	3	0.1405	0.1376
	4	0.1362	
	5	0.1383	
	6	0.1372	
	7	0.1377	
	8	0.1375	
1.0	1	0.1720	0.1608
	2	0.1514	0.1592
	3	0.1638	0.1591
	4	0.1563	
	5	0.1607	
	6	0.1581	
	7	0.1597	
	8	0.1593	
	9	0.1589	

Table 4.8 Sandwich plates comparison with experimental results (G_c=12670psi)
A - $G_f$not considered B - $G_f$considered

Side of plate	Core thickness	R_0	Experimental u_3 in.	Present u_3 in.
44.20	.514	.5408	0.168	A 0.166306 B 0.154612
	.390	.7211	0.359	A 0.30183 B 0.29141
32.04	.507	.7211	0.072	A 0.0699 B 0.0603
	.381	.7211	0.112	A 0.1119 B 0.1003
28.04	.503	.5768	0.035	A 0.03500 B 0.02891
	.388	.7211	0.065	A 0.6757 B 0.05805
21.97	.513	1.803	0.046	A 0.0443 B 0.0329
	.390	1.082	0.044	A 0.0417 B 0.03278

Table 4.9 Sandwich plates comparison with experimental results (G_c=5840psi)
A - $G_f$not considered B - $G_f$considered

Side of plate	Core thickness	R_0	Experimental u_3 in.	Present u_3 in.
44.20	.755	.721	0.110	A 0.1288 B 0.1024
	.637	.721	0.158	A 0.1691 B 0.1398
32.04	.751	.721	0.078	A 0.07748 B 0.05717
	.632	.721	0.087	A 0.1025 B 0.0790
28.04	.753	.721	0.024	A 0.02811 B 0.01692
	.635	.721	0.030	A 0.03678 B 0.02349
21.97	.754	2.884	0.039	A 0.05285 B 0.02563
	.636	2.163	0.037	A 0.05068 B 0.02646

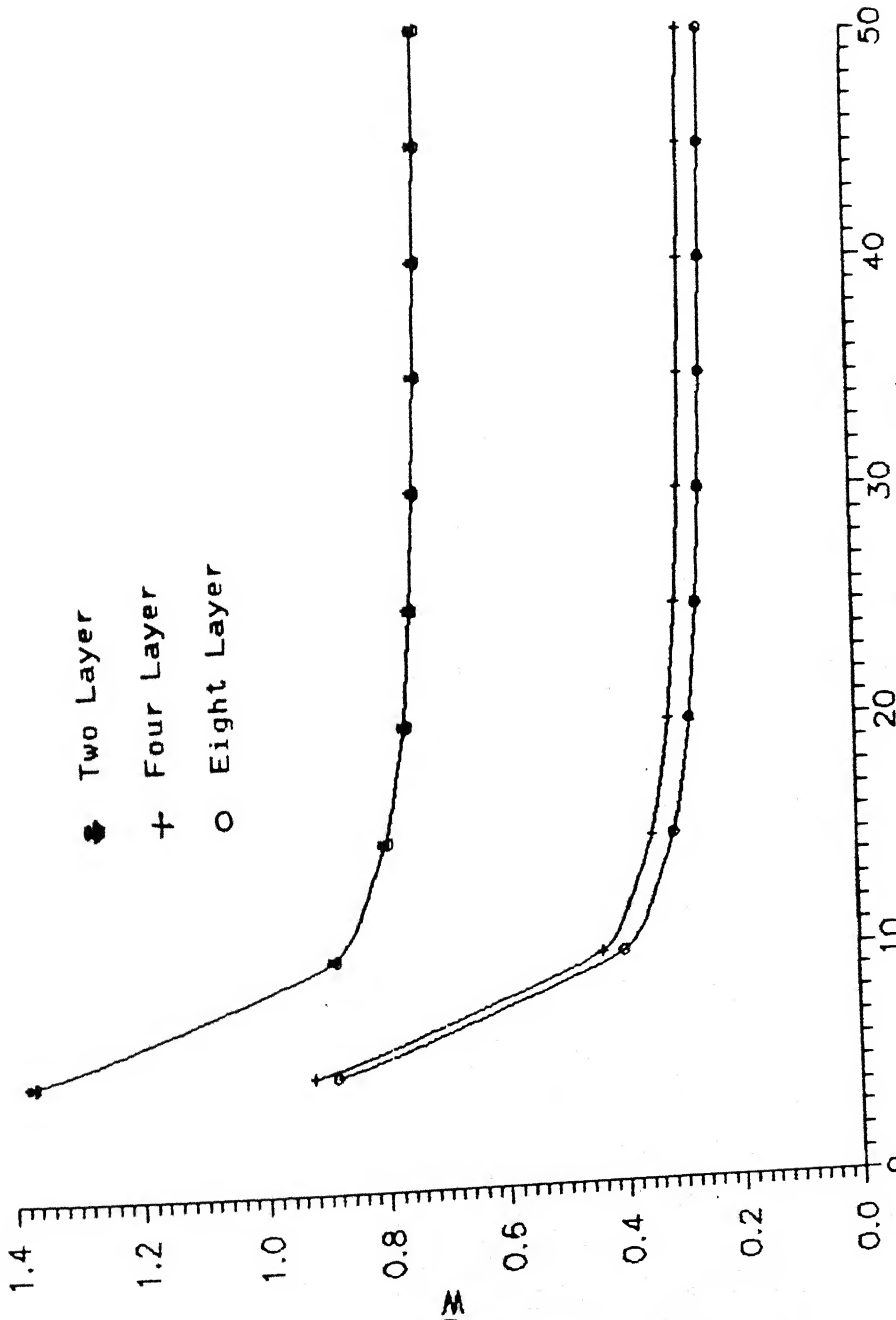

Fig. 4.1 Nondimensionalized centre deflections $\bar{W}$ versus side to thickness ratio for antisymmetric angle-ply (-45/45/...) square laminate under uniform transverse load.

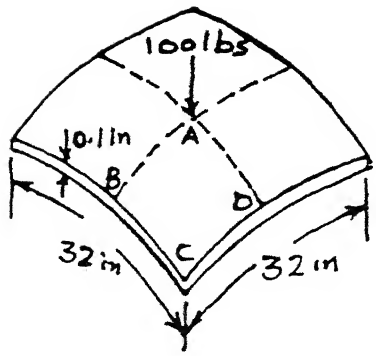

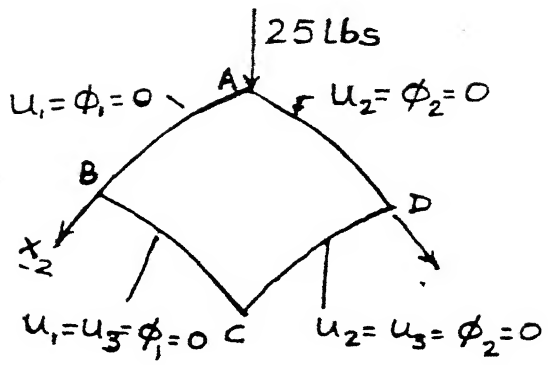

Fig. 4.2(a) Linear analysis of spherical shell

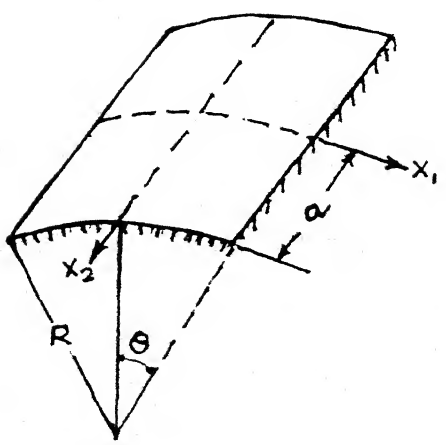

h = 3.175 mm

R = 2540 mm

a = 254 mm

θ = 0.1 rad

E = 3103 N/mm^2

ν = 0.3

Fig. 4.2(b) Bending of clamped, isotropic cylindrical shell

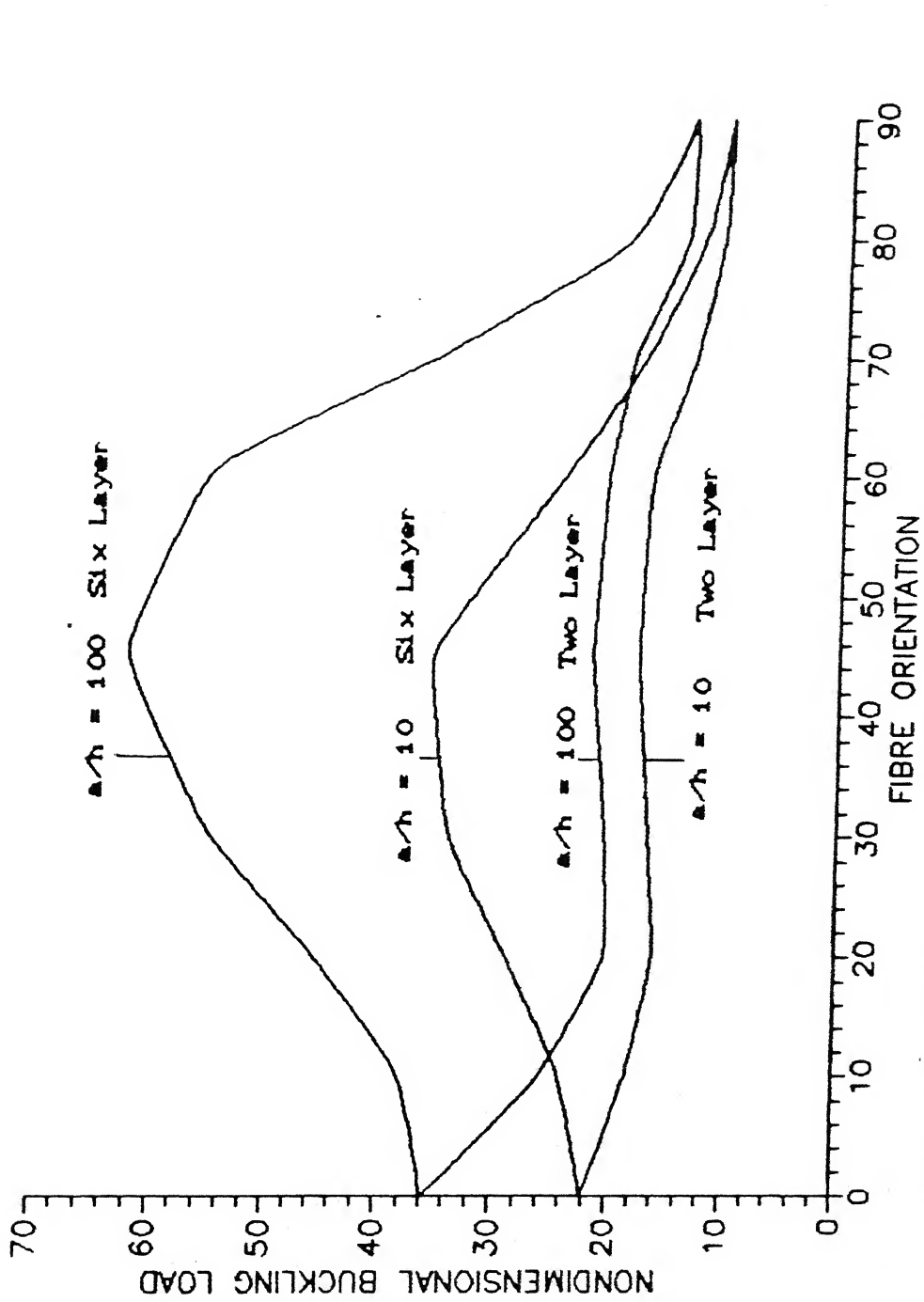

Fig. 4.3 Nondimensional buckling loads versus fibre orientation for antisymmetric angle-ply $(\alpha/-\alpha/\ldots)$ square laminate

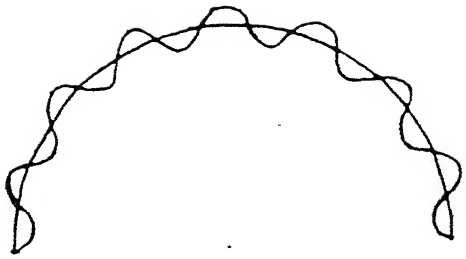

Fig. 4.4(a) Buckling of cylindrical shell

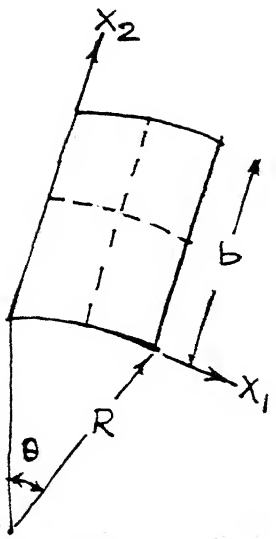

$\theta = 12^{\circ}$

R = 36 in.

b = 6.5 in.

Fig. 4.4(b) Finite elemnet idealization for buckling analysis.

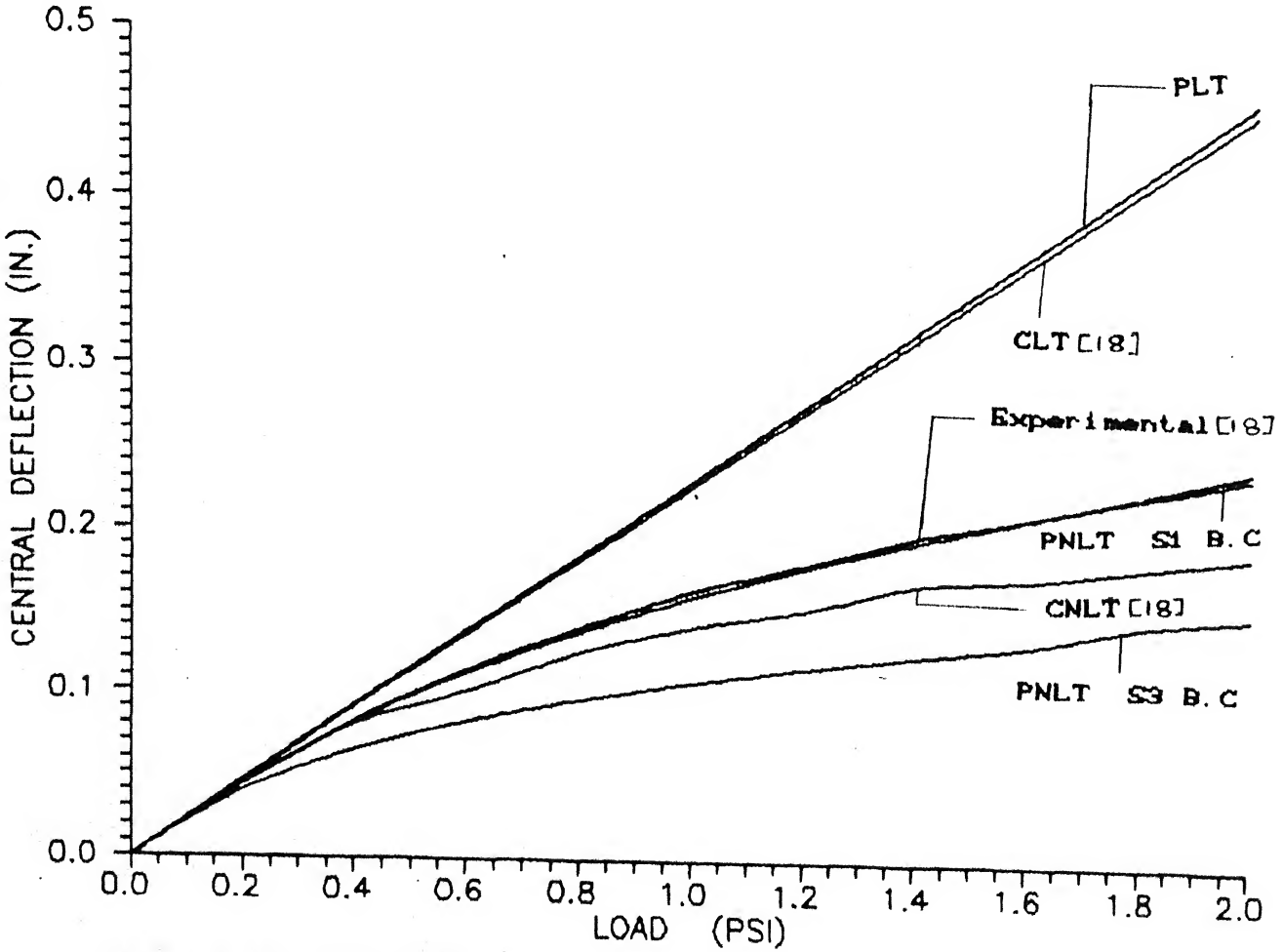

Fig. 4.5 Load deflection curve for orthotropic laminate under uniform transverse load

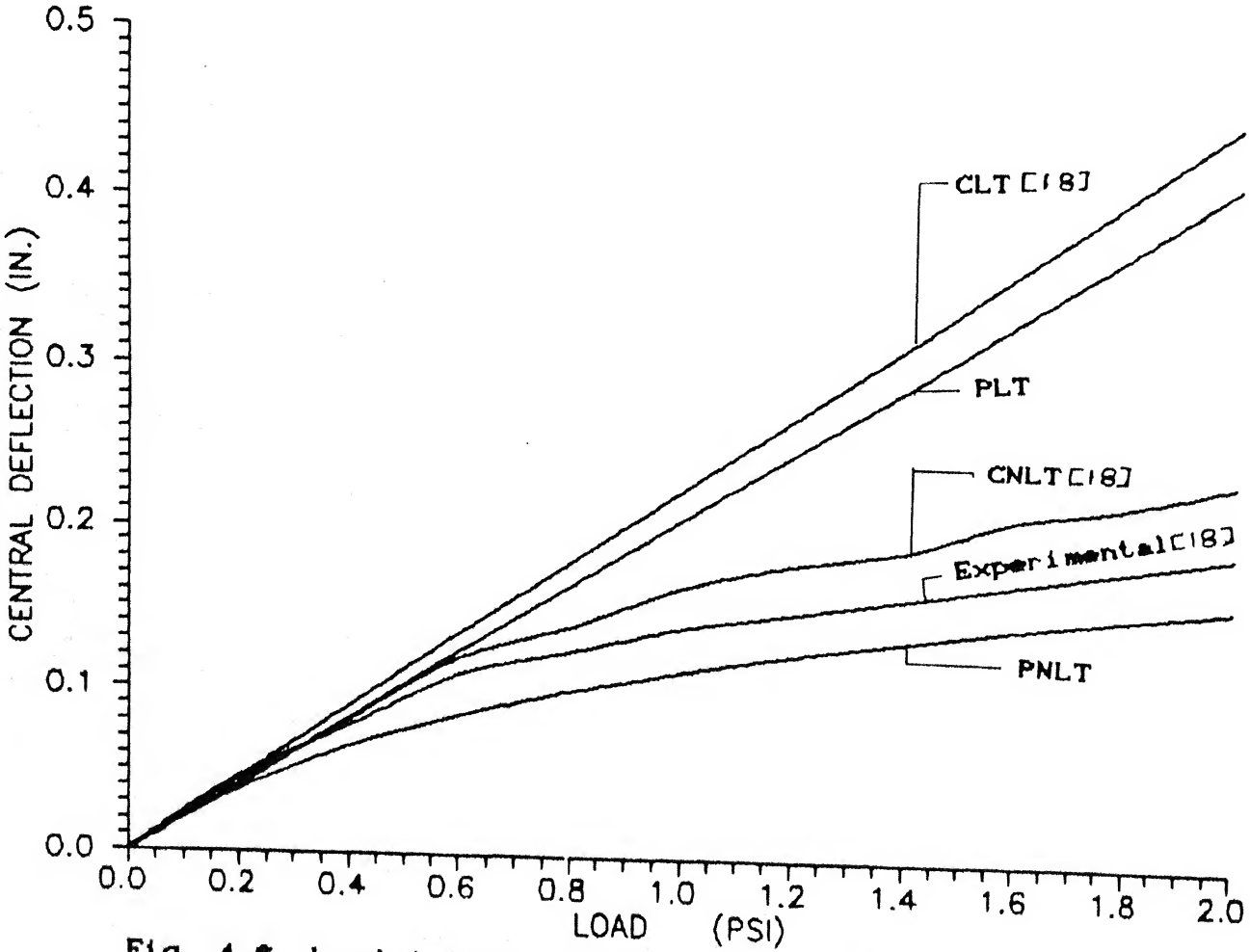

Fig. 4.6 Load deflection curve for cross-ply laminate under uniform transverse load

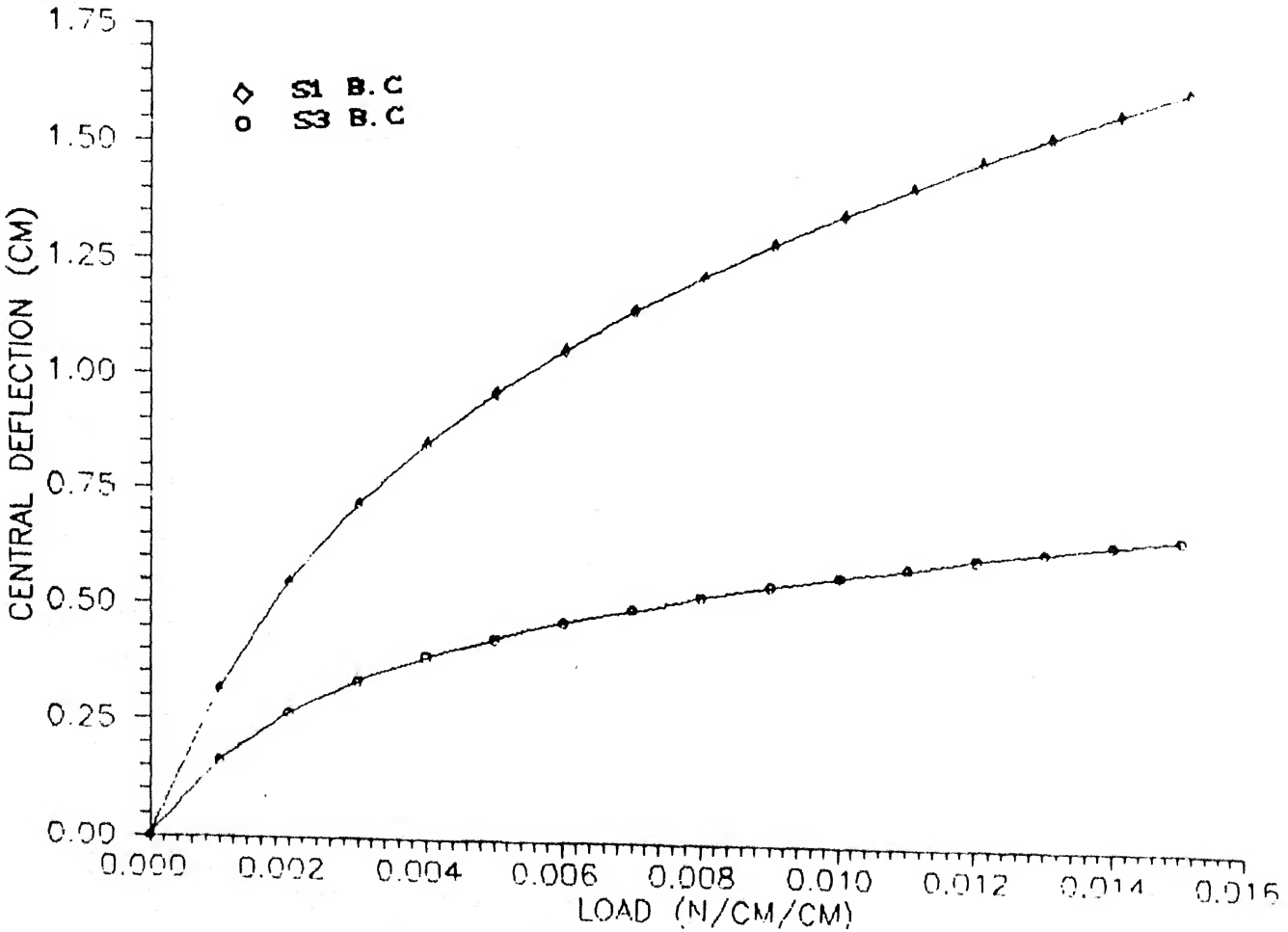

Fig. 4.7 Bending of cross-ply (0/90), simply supported, square laminate

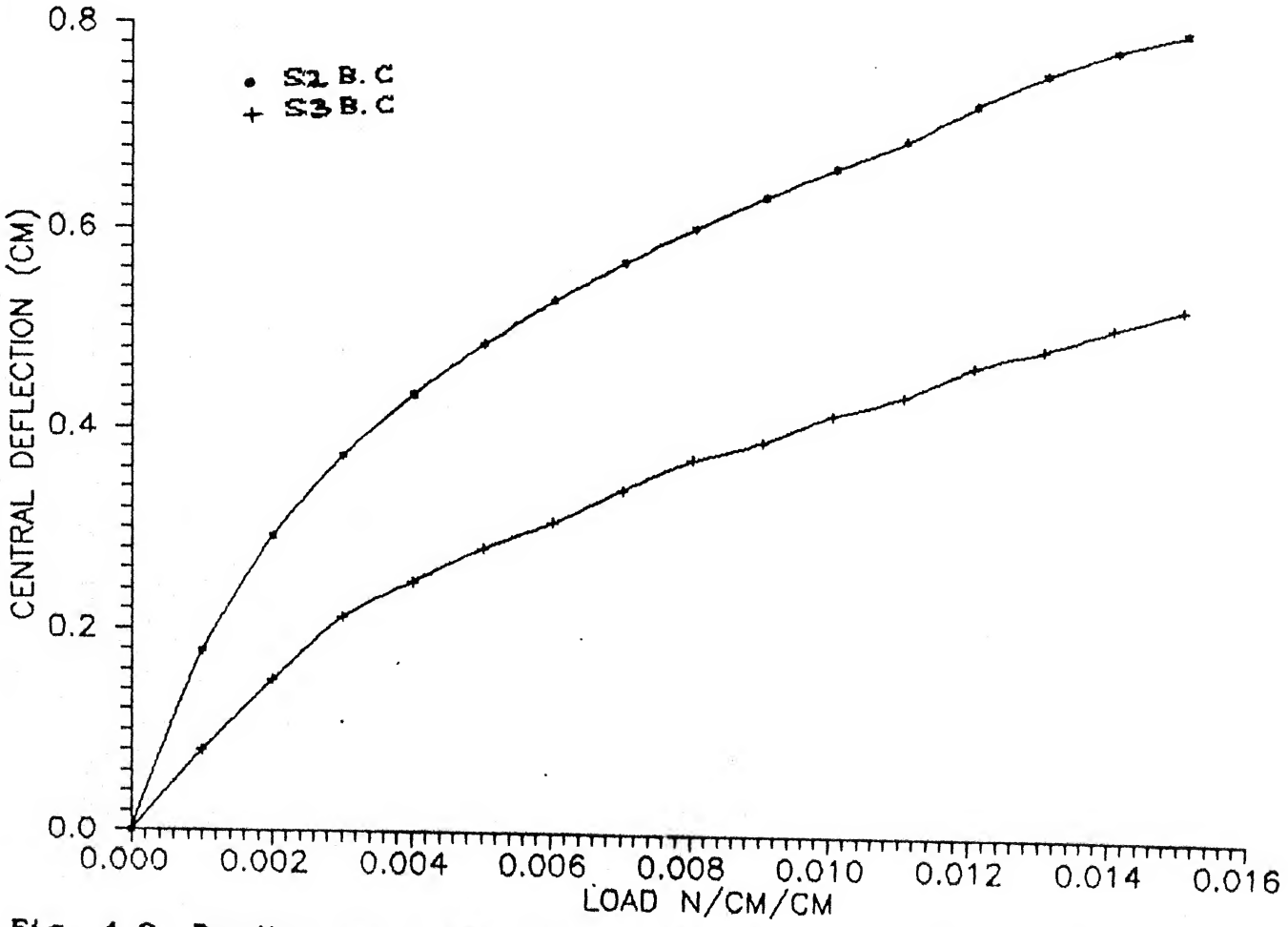

Fig. 4.8 Bending of angle-ply (-45/45), simply supported, square laminate

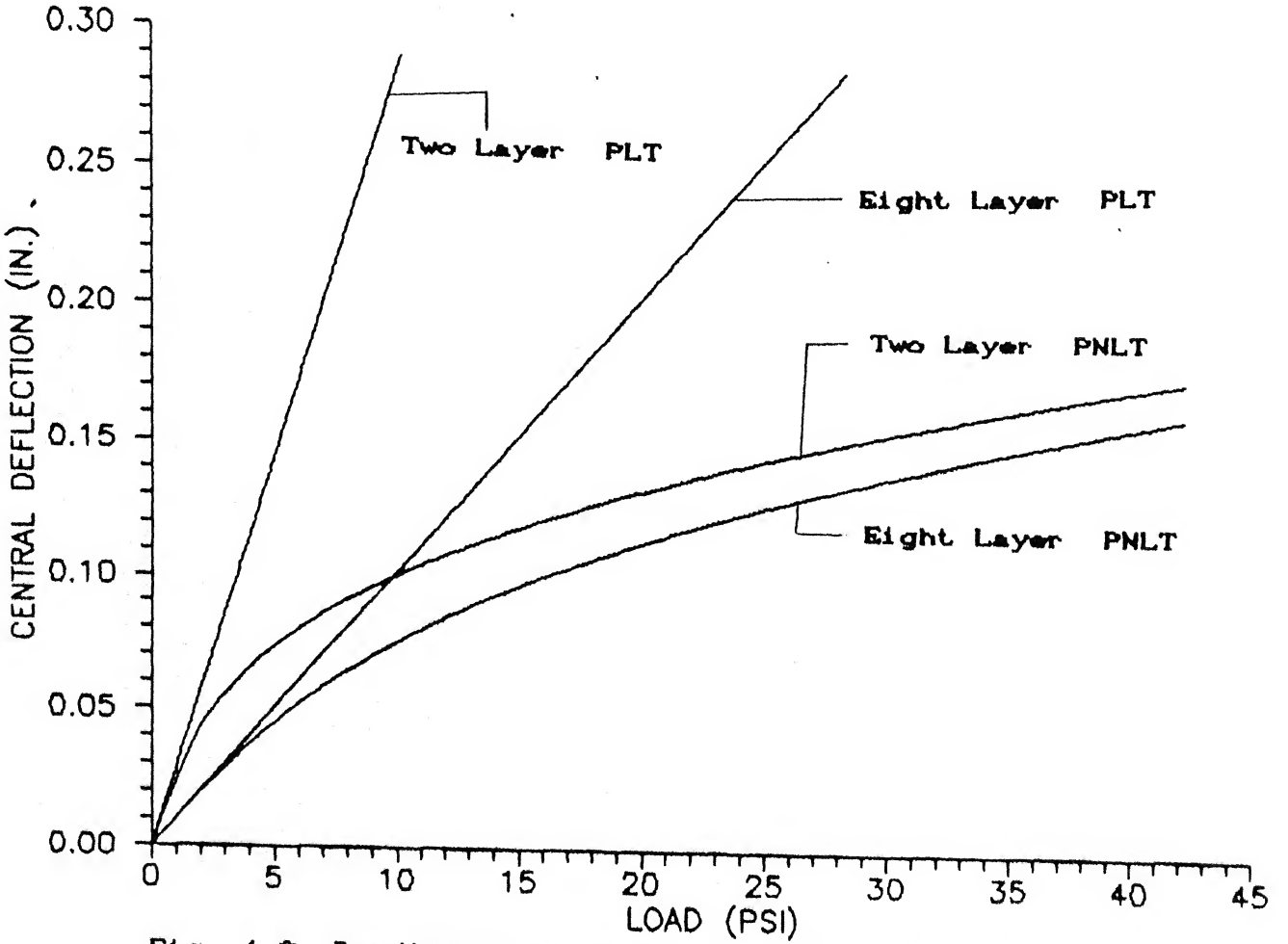

Fig. 4.9 Bending of cross-ply (0/90), clamped square laminate

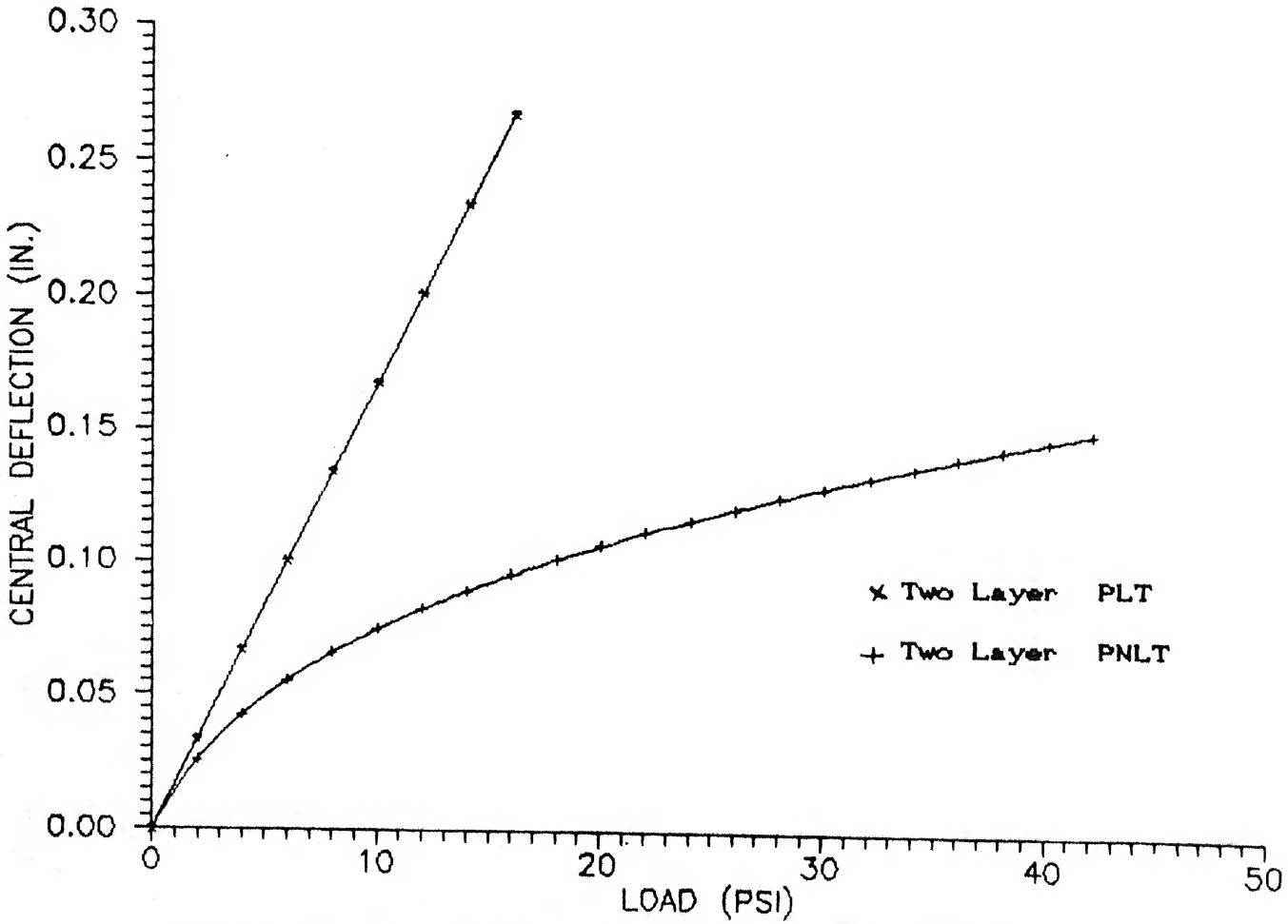

Fig. 4.10 Bending of angle-ply (-45/45), clamped square laminate

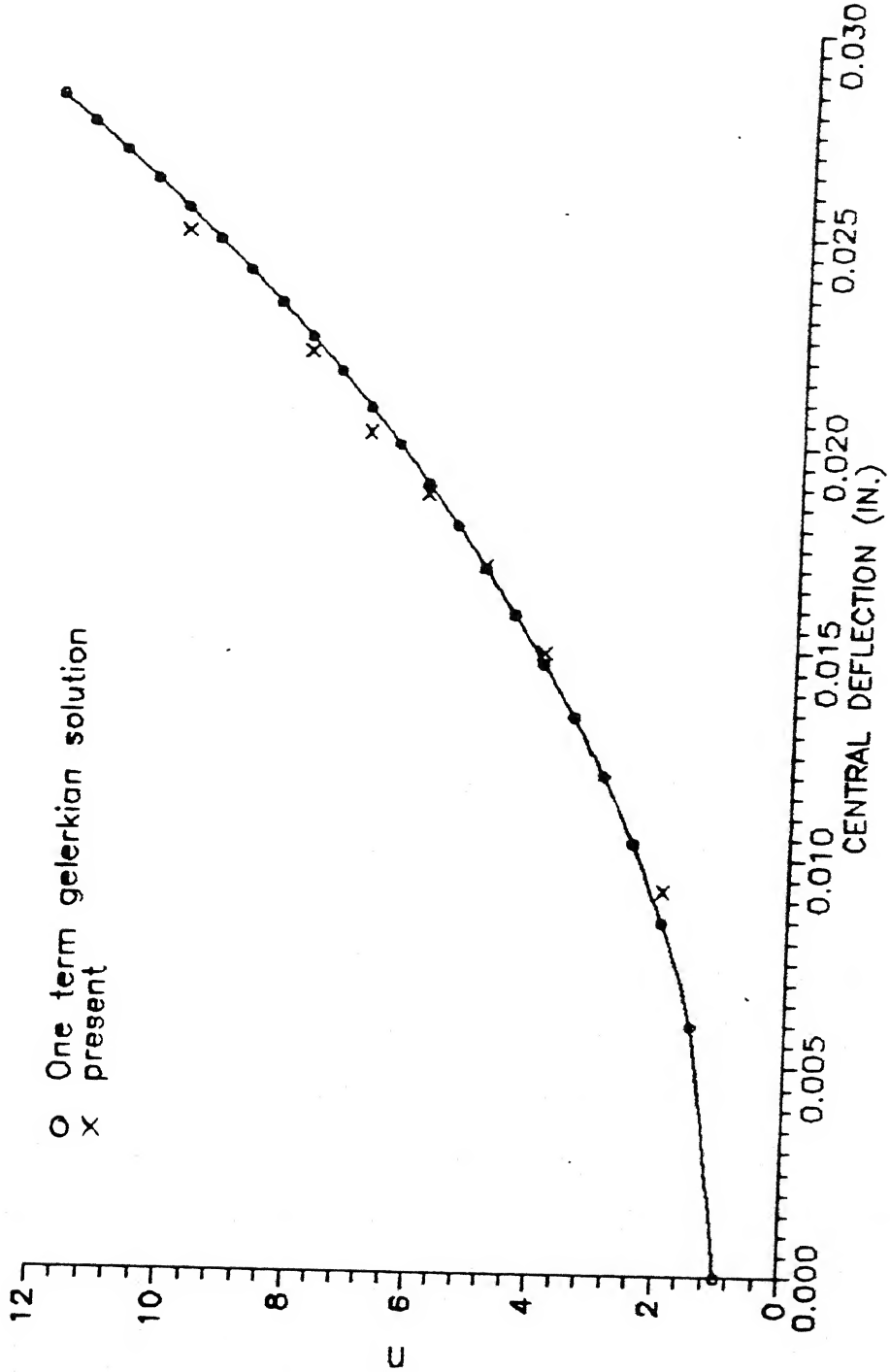

Fig. 4.11 Post buckling of isotropic plate

CHAPTER 5

CONCLUSIONS

5.1 Conclusions :

A first order shear deformation theory for the nonlinear bending, post buckling of plates, linear bending and buckling of shells is presented. On the basis of the limited study carried pout the following conclusions can be drawn.

1) It is clear from the Table 4.1 that the type of integration scheme has a little effect on the nine noded lagrangian element. It is also evident that one has to use reduced integration for the shear terms in the thin plate region to circumvent locking.

2) It can be seen from the Table 4.2 that FSDT results are not reliable for a/h < 10 for the bending problems. For a/h > 10 there is no significant difference between FSDT and HSDT results.

3) The FSDT results for the uniaxial buckling load are studied for three layered symmetric cross-ply and is given in Table 4.6. For this type of laminate studied it can be seen that present results are very close to HSDT results for all thickness ratios. It can be concluded that the present theory is adequate to determine the lowest buckling load. The classical plate theory is not reliable for a/h < 20.

4) It can be seen from the Table 4.7 that Newton-Raphson method is more efficient than the picard type of iteration through the former involves computation of derivative of the stiffness

matrix.

5) As seen from the Fig. 4.4 it can be concluded that the present nonlinear results are close to the experimental results with S1 boundary condition than S3 boundary condition. The difference in results for S1 and S3 boundary conditions is due to the bending-stretching coupling introduced through the nonlinearity. The linear results over estimate the deflections and are not reliable where the deflections are of the order of the thickness. It can noted that the experimental boundary conditions may lie in between S1 and S3 boundary conditions for an orthotropic plate.

6) Due the bending stretching coupling the different in plane boundary conditions (S1,S2,S3) give different results. Of all the boundary conditions S3 is stiffening type. This can be seen from Fig. 4.7 and 4.8.

7) From Fig. 4.9 and 4.10 it can seen that cross-ply exhibits higher nonlinearity than angle-ply laminates. It can also noted that for the cross-ply as the number of layers is increased the nonlinearity is decreasing.

5.2 Recommendations for the Future Work :

Some of the future work that can be carried out as an extension or improvement over the present investigation are suggested below.

The buckling formulation and program that is developed can be utilized to analyze the stability of sandwich plates. The program developed here also caters for biaxial and shear buckling

of laminated composite plates. This could be investigated for future work.

With the little effort this work can be extended to nonlinear analysis by taking all the nonlinear terms in the strain displacement relation as

$$\epsilon_1^o = \frac{\partial u_1}{\partial x_1} + \frac{1}{2}\left[\left(\frac{\partial u_1}{\partial x_1}\right)^2 + \left(\frac{\partial u_1}{\partial x_1}\right)^2 + \left(\frac{\partial u_1}{\partial x_1}\right)^2\right]$$

There will be additional matrices such as $[B]^{o^e}$ give in Eqn.(3.). This becomes computationally expensive. One can investigate whether that effort is required in engineering design.

The post buckling problem done in the present work is limited to some special boundary conditions. By adding an additional external potential term one can solve it for all boundary conditions.

BIBLIOGRAPHY

1. Stavsky,Y.,"On the theory of symmetrically heterogeneous plates having the same thickness variation of elastic moduli" Topics in Applied Mechanics (Abir.,D.,Ollendorff,F.,and Riner,.M.,eds),American Elsevier (1965)

2. Yang,P.C.,Norris,C.H.,and Stavsky,Y.,"Elastic wave propogation in heterogeneous plates",Intl.J.Solids Struct.,2,pp 665-684 (1966)

3. Pagano,N.J,"Exact solutions for rectangular bidirectional composites and sndwitch plates",J.Composit matls.,4,pp 20-34 (1970)

4. Sun,C.T and Whitney,J.M.,"Theories for the dynamic response of laminated plates", AIAA J.,11,pp 178-183(1973)

5. Srinivas,s. and Rao,A.K.,"Bending vibration and buckling of simply supported thick orthotropic rectangular plates and laminates",Intl.J.Solids Struc.,6,pp 1463-1481 (1970)

6. Whitney,J.M.and Pagano,N.J.,"Shear deformation in heterogenious anisotrpic plates', J.Appl.Mechanics, Trans. ASME, 37, pp 1031-1036 (1970)

7. Sinha,P,K.and Rath,A.K.,"Vibration and buckling of cross-ply laminated circular cylindrical pannels",Aeronaut.Quart.,26,pp 211-218 (1975)

8. Pryor,C.W.Jr. and Barker,R.M.,"A finite element analysis including transverse shear effects for application to laminated plates",AIAA J.,9,pp912-917 (1971)

9. Pica.A,Wood,R.D.and Hinton.E.,"Finite element analysis of geometrically nonlinear plate behavior using a mindilin formulation Computers Stuct.,11, pp 203-215 (1980)

10. Reddy,J.N. ,"A penalty plate bending elment for the analsis of laminated anisotropic composite plates", Intl. J. Numer. Methods. eng ,15,pp 1187-1206 (1980)

11. Reddy,J.N.and Chao,W.C.,"A comparision of closed form and finite element solutions of thick laminated anisotropic rectangular plates",Nuclear Engr. Des.,64, pp 153-167 (1981)

12. Reddy,J.N.,"A note on symmetry considerations in the transient response of unsymmetrically laminated composite plates", Intl.J.Numer.Methods engr.,20, pp 175-194 (1984)

13. Hass, D.J.,and Lee,S.W., "A nine noded assumed strain finite element for composite plates and shells", Computers Struct., 26, (3), pp 445-452 (1987)

14. Zienkiwicz,O.C., "The finite element method ", third ed., Mchgraw - Hill, London (1977)

15. Cook, R.D., "Concepts and applications of finite element analysis ", 2nd ed., Wiley, New York , (1981)

16. Phan,N.D.,and Reddy,J.N., " Analysis of laminated composite plates using a higher order shear deformation theory ", Intl.J.Numer.Methods.Engr.,21, pp 2201-2219 (1985)

17. Phan,N.D.,and Reddy,J.N.,"Stability and vibration of isotropic, orthotropic and laminated plates according to higher order shear deformation theory ", J.Sound. and Vib.,,98, (2), pp 157-170 (1985)

18. Zaghloul, S.A.,and Kennedy, J.B., "Nonlinear behavior of symmetrically laminated plates ", Intl. J. Appl. Mech., 22 , pp 234-236 (1975)

19. Sanders,J.L.Jr.,"An improved first approximation theory for thin shells",NASA TR R-24, June 1959

20. Reddy,J.N.,"An introduction to finite element method ", Mc-Graw Hill New york (1984)

21. Reddy.,J.N.,"Energy and variational methods in applied mechanics ",John Wiley & sons., (1984)

22. Gajbir Singh and Sadasiva Rao, Y..K.,"Stability of thick angle-ply composite plates ", Computer Struct.,29, (2), pp 317-322 (1988)

23. Chandra,R.,and Raju,B.B.,"Large amplitude flexural vibrations of cros-ply laminated composite plates ",Fibre.Sci.Tech.,8, pp 243-263 (1975)

24. Chia,C.Y.,and Prabhakara,M.K.,"A general mode approach to nonlinear flexural vibrations of laminated rectangular plates," J.Appl..Mechanics,Trans.ASME, 45 , pp 623-628 (1978)

25. Mallet, R.,and Marcal, P.V., "Finite element analysis of nonlinear structures ", J. Struct. Div.,ASCE, 94, pp 2081-2105 (1968)

26. Zienkiewitcz, O.C. and Nayak,G.C., "A general approach to problems of plasticty and large deformations using isoparametric elements ", Proc. Conf. Matrix Methods in Engr., 17, pp 635-642 (1978)

27. Wood, R.D., and Scarefler, B., "Geometric nonlinear analysis - A correlation of finite element notations ", Intl.J. Numer. Methods. Engr., 17, pp 635-642 (1978)

28. Reddy,J..N.,and Chao,W.C.,"Non linear bending of thick rectangular laminated composite plates ",Intl.J.Nonlin. Mechanics(1981)

29. Pucha,N.S.,andReddy,J.N.,"A refined mixed shear flexible finite element for the nonlinear analysis of laminated plates " , Computers Stuc.,22 (2), pp 529-538

30. Ambartsumyan,S.A.,"Theory of anisotropic shells",Moscow, 1961, English Translation,NASA TT-F-118 (May 1964)

31. Dong,S.B.,Pister,K.S.,and Taylor,R.L.,"On the theory of laminated anisotropic shells and plates ",J.Aerospace.Sci., 29 pp 969-975 (1962)

32. Cheng,S.and Ho,B.P.C.,"Stability of heterogeneous anisotropic cylindrical shells under combined loading" AIAA J., 1(4), pp 892-898 (1963)

33. Flugge,W.,"Stresses in shells " Spinger verlag Berlin (1960)

34. Zukas,J.A.,and Vinson,J.R.,"Laminated transversly isotropic cylindrical shells ",J.Appl.Mechanics,41, pp 471-476 (1974)

35. Pandya.S.C.,and Natarajan,"Finite element analysis of laminated shells of revolution ", Computers Stuc., 6, pp 61-64

36. Shivakumar.K.N.,and Krishnamurthy,A.V.,"A high precision ring element for vibration of laminated shells ",J.Sound and Vib., 58 (3), pp 311-318 (1978)

37. Rao,K.P.,"A rectangular laminated anisotropic shallow thin shell finite element ",Compuuter Methods In Appl.Mechanics and Engr.,15, pp 13-33 (1978)

38. Reddy,J.N.,"Bending of laminated anisotropicshells by a shear deformable finite element",Fiber.Sci.Tech.,17, pp 9-24 (1982)

39. Reddy,J.N.,and Chandrashekhara,K.,"Geometrically non linear transient analysis of doubly curved shells "Intl.J.Nonlin. Mechanics , 20 (2),pp 79-90 (1985)

40. Chandrashekara,K.,"General nonlinear bending analysis of composite beams plates and shells " Proc.,Int.Conf. on Composite Mat. and Struc.(eds) Pandalai,K.A.V.,and Malhotra, S.K., Tata Mc-Graw Hill ,New Delhi pp 392-399

41. Jones,R.M.,"Mechanics of composite materials ", Mc-Graw Hill New York (1975)

42. Timeshenko,S.,and Gere,J.M.,"Theory of elastic stability ", Second ed.,Mc-Graw Hill New York ,1961

43. Bathe,K.J.,and Wilson,E.L.,"Numerical methods in finite element analysis ", Prentice-Hall of India pvt Ltd,New Delhi (1987)

44. Allen,H.G.,"Analysis and design of structural sandwich panels" ,Pargamon Press, London (1969)

APPENDIX I

1 Introduction :

A composite laminate is composed by bonding together a number of lamina. In each lamina material axes may not coincide with the reference axes. The material constants of a lamina which are functions of engineering constants and orientation of fibre α are given in the following section.

2 Description :

The stress strain relations for a lamina, with material axes coinciding with reference axes and assuming the transverse stress is negligible, are given by

$$\begin{Bmatrix} \sigma_1 \\ \sigma_2 \\ \sigma_6 \\ \sigma_4 \\ \sigma_5 \end{Bmatrix} = \begin{bmatrix} Q_{11} & Q_{12} & 0 & 0 & 0 \\ & Q_{22} & 0 & 0 & 0 \\ & & Q_{66} & 0 & 0 \\ & \text{Sym} & & Q_{44} & 0 \\ & & & & Q_{55} \end{bmatrix} \begin{Bmatrix} \epsilon_1 \\ \epsilon_2 \\ \epsilon_6 \\ \epsilon_4 \\ \epsilon_5 \end{Bmatrix} \qquad \text{(A 1.1)}$$

Where

$$Q_{11} = \frac{E_1}{1-\nu_{12}\nu_{21}} \quad ; \quad Q_{22} = \frac{E_2}{1-\nu_{12}\nu_{21}}$$

$$Q_{12} = \frac{E_1\nu_{21}}{1-\nu_{12}\nu_{21}} = \frac{E_2\nu_{12}}{1-\nu_{12}\nu_{21}}$$

$$Q_{66} = G_{12} \quad ; \quad Q_{44} = G_{23} \quad ; \quad Q_{55} = G_{13} \qquad \text{(A 1.2)}$$

For an arbitrarily oriented laminated lamina after carrying out necessary transformation stress-strain relations are given by,

$$\begin{Bmatrix} \sigma_1 \\ \sigma_2 \\ \sigma_6 \\ \sigma_4 \\ \sigma_5 \end{Bmatrix} = \begin{bmatrix} \bar{Q}_{11} & \bar{Q}_{12} & \bar{Q}_{16} & 0 & 0 \\ & \bar{Q}_{22} & \bar{Q}_{26} & 0 & 0 \\ & & \bar{Q}_{66} & 0 & 0 \\ & \text{Sym} & & \bar{Q}_{44} & \bar{Q}_{45} \\ & & & & \bar{Q}_{55} \end{bmatrix} \begin{Bmatrix} \epsilon_1 \\ \epsilon_2 \\ \epsilon_6 \\ \epsilon_4 \\ \epsilon_5 \end{Bmatrix} \qquad \text{(A 1.3)}$$

Where

$$\begin{aligned}
\bar{Q}_{11} &= Q_{11}C^4 + 2\left(Q_{12} + 2Q_{66}\right)S^2C^2 + Q_{22}S^4 \\
\bar{Q}_{12} &= \left(Q_{11} + Q_{22} - 4Q_{66}\right)S^2C^2 + Q_{12}\left(S^4 + C^4\right) \\
\bar{Q}_{16} &= \left(Q_{11} - Q_{12} - 2Q_{66}\right)C^3S + \left(Q_{12} - Q_{22} + 2Q_{66}\right)S^3C \\
\bar{Q}_{22} &= Q_{11}S^4 + 2\left(Q_{12} + 2Q_{66}\right)S^2C^2 + Q_{22}C^4 \\
\bar{Q}_{26} &= \left(Q_{11} - Q_{12} - 2Q_{66}\right)S^3C + \left(Q_{12} - Q_{22} - 2Q_{66}\right)C^3S \\
\bar{Q}_{44} &= Q_{44}C^2 + Q_{55}S^2 \\
\bar{Q}_{45} &= \left(Q_{55} - Q_{44}\right)CS \\
\bar{Q}_{55} &= Q_{44}S^2 + Q_{55}C^2
\end{aligned} \qquad \text{(A 1.4)}$$

In which C= COS(α) and S = SIN(α) and α is the angle between reference axes and principal orthotropic axes

APPENDIX II

1. Derivation of Tangent Stiffness Matrix :

Substituting the Eqn. (3.20) , in to Eqn. (3.25) enables the tangent stiffness matrix K_T to be written as

$$[K_T] = \int_A [B]^{e^T} L(\bar{N}) + M(\bar{N})[B]^e + [C]^{e^T} L(\bar{M}) + [D]^{e^T} L(\bar{Q}) \qquad \text{(A 2.1)}$$

Where

$$L(\bar{N}) = \begin{bmatrix} \frac{\partial N_1}{\partial \delta_1} & \frac{\partial N_1}{\partial \delta_2} & \cdots & \frac{\partial N_1}{\partial \delta_N} \\ \frac{\partial N_2}{\partial \delta_1} & \frac{\partial N_2}{\partial \delta_2} & \cdots & \frac{\partial N_2}{\partial \delta_N} \\ \frac{\partial N_6}{\partial \delta_1} & \frac{\partial N_6}{\partial \delta_2} & \cdots & \frac{\partial N_6}{\partial \delta_N} \end{bmatrix} \qquad \text{(A 2.2)}$$

$$M(\bar{N}) = \begin{bmatrix} N_1 \dfrac{\partial}{\partial \delta_1} & N_2 \dfrac{\partial}{\partial \delta_1} & N_6 \dfrac{\partial}{\partial \delta_1} \\ N_1 \dfrac{\partial}{\partial \delta_2} & N_2 \dfrac{\partial}{\partial \delta_2} & N_6 \dfrac{\partial}{\partial \delta_2} \\ \cdot & \cdot & \cdot \\ \cdot & \cdot & \cdot \\ \cdot & \cdot & \cdot \\ N_1 \dfrac{\partial}{\partial \delta_N} & N_2 \dfrac{\partial}{\partial \delta_N} & N_6 \dfrac{\partial}{\partial \delta_N} \end{bmatrix} \qquad \text{(A 2.3)}$$

$$L(\bar{M}) = \begin{bmatrix} \dfrac{\partial M_1}{\partial \delta_1} & \dfrac{\partial M_1}{\partial \delta_2} & - - - - - - - & \dfrac{\partial M_1}{\partial \delta_N} \\ \dfrac{\partial M_2}{\partial \delta_1} & \dfrac{\partial M_2}{\partial \delta_2} & - - - - - - - & \dfrac{\partial M_2}{\partial \delta_N} \\ \dfrac{\partial M_6}{\partial \delta_1} & \dfrac{\partial M_6}{\partial \delta_2} & - - - - - - - & \dfrac{\partial M_6}{\partial \delta_N} \end{bmatrix} \qquad \text{(A 2.4)}$$

$$L(\bar{Q}) = \begin{bmatrix} \dfrac{\partial Q_1}{\partial \delta_1} & \dfrac{\partial Q_1}{\partial \delta_2} & - - - - - - - & \dfrac{\partial Q_1}{\partial \delta_N} \\ \dfrac{\partial Q_2}{\partial \delta_1} & \dfrac{\partial Q_2}{\partial \delta_2} & - - - - - - - & \dfrac{\partial Q_2}{\partial \delta_N} \end{bmatrix} \qquad \text{(A 2.5)}$$

Where N denotes total degree of freedom.

Since the stress resultants are linear function of strain $\{\in\}$ the variation of stress resultants N_i can be writen from Eqn.(2.7) as,

expression for the tangent stiffness matrix as

$$[K]_T = \int_A \Big[[B]^{o\,e^T} [QA] [B]^{o\,e} + [B]^{o\,e^T} [QB] [C]^e + M(\bar{N}) \Big[[B]_L^{o\,e} + [E]^e [G]^e \Big] + [C]^{e^T} [QB] [B]^{o\,e} + [C]^{e^T} [QD] [C]^e + [D]^{e^T} [QS] [D]^e \Big] dA \qquad \text{(A 2.8)}$$

Considering the third integral in Eqn. (A 2.8) and noting that $[B]^{o\,e}$ is not a function of δ gives, upon multipication of $M(\bar{N})$ and E

$$\int_A M(N) [B]^{o\,e} dA =$$

$$\int_A \begin{bmatrix} N_1 \dfrac{\partial\left(\frac{\partial u_3}{\partial x_1}\right)}{\partial \delta_1} + N_6 \dfrac{\partial\left(\frac{\partial u_3}{\partial x_2}\right)}{\partial \delta_1} & N_2 \dfrac{\partial\left(\frac{\partial u_3}{\partial x_1}\right)}{\partial \delta_1} + N_6 \dfrac{\partial\left(\frac{\partial u_3}{\partial x_2}\right)}{\partial \delta_1} \\ N_1 \dfrac{\partial\left(\frac{\partial u_3}{\partial x_1}\right)}{\partial \delta_2} + N_6 \dfrac{\partial\left(\frac{\partial u_3}{\partial x_2}\right)}{\partial \delta_2} & N_2 \dfrac{\partial\left(\frac{\partial u_3}{\partial x_2}\right)}{\partial \delta_2} + N_6 \dfrac{\partial\left(\frac{\partial u_3}{\partial x_1}\right)}{\partial \delta_2} \\ N_1 \dfrac{\partial\left(\frac{\partial u_3}{\partial x_1}\right)}{\partial \delta_N} + N_6 \dfrac{\partial\left(\frac{\partial u_3}{\partial x_2}\right)}{\partial \delta_N} & N_2 \dfrac{\partial\left(\frac{\partial u_3}{\partial x_2}\right)}{\partial \delta_N} + N_6 \dfrac{\partial\left(\frac{\partial u_3}{\partial x_1}\right)}{\partial \delta_N} \end{bmatrix} G dA \qquad \text{(A 2.13)}$$

The differential with respect to δ in Eqn. (A 2.13) are the coefficients of [G] matrix of Eqn. (3.10d) typically for a degree of freedom i

$$\frac{\partial \left(\frac{\partial u_3}{\partial x_1} \right)}{\partial \delta_i} = G_{1i} \qquad \text{(A 2.14)}$$

and

$$\frac{\partial \left(\frac{\partial u_3}{\partial x_2} \right)}{\partial \delta_i} = G_{2i} \qquad \text{(A 2.15)}$$

Now $\int M (\bar{N}) [B]^{o e}$ can be written as

$$\int_A [G]^{e^T} \begin{bmatrix} N_1 & N_6 \\ N_6 & N_2 \end{bmatrix} [G]^e \, dA \qquad \text{(A 2.16)}$$

Consequently Eqn. (A 2.17) may be reaaranged to give the expressions for K_T shown in Eqn (3.27a)

AE-1990-M-VEN-STU